New Specimens of *Anchiornis huxleyi* (Theropoda: Paraves) from the Late Jurassic of Northeastern China

Rui Pei, Quanguo Li, Qingjin Meng, Mark A. Norell, and Ke-Qin Gao

Bulletin of the American Museum of Natural History

NEW SPECIMENS OF *ANCHIORNIS HUXLEYI* (THEROPODA: PARAVES) FROM THE LATE JURASSIC OF NORTHEASTERN CHINA

RUI PEI
Department of Earth Sciences, the University of Hong Kong, Hong Kong;
Division of Paleontology, American Museum of Natural History

QUANGUO LI
State Key Laboratory of Biogeology and Environmental Geology,
China University of Geosciences, Beijing

QINGJIN MENG
Beijing Museum of Natural History, Beijing

MARK A. NORELL
Division of Paleontology, American Museum of Natural History

KE-QIN GAO
School of Earth and Space Sciences, Peking University, Beijing

BULLETIN OF THE AMERICAN MUSEUM OF NATURAL HISTORY
Number 411, 66 pp., 40 figures, 1 table
Issued April 13, 2017

Copyright © American Museum of Natural History 2017 ISSN 0003-0090

CONTENTS

Abstract 4
Introduction 4
Material 5
Morphological Description 6
Skull and Mandible 6
Premaxilla 6
Maxilla 10
Nasal 17
Frontal 18
Lacrimal 18
Jugal 19
Postorbital 19
Quadratojugal 19
Quadrate 19
Squamosal 20
Palatal elements 20
Braincase 20
Dentary 21
Splenial 22
Angular 22
Surangular 22
Prearticular 23
Articular 23
Postcranium 23
Cervical vertebrae 23
Dorsal vertebrae 24
Sacral vertebrae 29
Caudal vertebrae 29
Pectoral girdle 32
Humerus 34
Ulna and radius 35
Carpals 36
Manus 37
Ilium 40
Pubis 42
Ischium 42
Femur 46
Tibiotarsus 46
Pes 47
Plumage 51
Discussion 53
Identity of New Specimens as *Anchiornis huxleyi* and Diagnosis of the Taxon 53
Affiliation of *Anchiornis huxleyi* 54
Affiliation to Maniraptora and Paraves 54

Comparison with *Archaeopteryx* 55
Comparison with Troodontidae 55
Comparison with Deinonychosauria 56
Variation within Specimens of *Anchiornis huxleyi* 57
Comparisons with *Pedopenna, Xiaotingia, Eosinopteryx,* and *Aurornis* 58
Summary 60
Acknowledgments 60
References 60
Appendix 1. Abbreviation List 65

ABSTRACT

Four new specimens of *Anchiornis huxleyi* (PKUP V1068, BMNHC PH804, BMNHC PH822, and BMNHC PH823) were recently recovered from the Late Jurassic fossil beds of the Tiaojishan Formation in northeastern China. These new specimens are almost completely preserved with cranial and postcranial skeletons. Morphological features of *Anchiornis huxleyi* have implications for paravian character evolution and provide insights into the relationships of major paravian lineages. *Anchiornis huxleyi* shares derived features with avialans, such as a straight nasal process of the premaxilla and the absence of an external mandibular fenestra in lateral view. However, *Anchiornis huxleyi* lacks several derived deinonychosaurian features, including a laterally exposed splenial and a specialized raptorial pedal digit II. Morphological comparisons strongly suggest *Anchiornis* is more closely related to avialans than to deinonychosaurians or troodontids. *Anchiornis huxleyi* exhibits many conservative paravian features, and closely resembles *Archaeopteryx* and other Jurassic paravians from Jianchang County, such as *Xiaotingia* and *Eosinopteryx*. The other Jianchang paravian, *Aurornis xui*, is likely a junior synonym of *Anchiornis huxleyi*.

INTRODUCTION

The Late Jurassic fossil beds of western Liaoning Province and nearby areas have revealed a plethora of extraordinary fossil invertebrates and vertebrates over the past several years (Zhang, 2002; Sullivan et al., 2014). In addition to many fossil mammals (Meng et al., 2006; Luo et al., 2007a, 2007b, 2011; Zhou et al., 2013), pterosaurs (Ji and Yuan, 2002; Lü et al., 2009), salamandroids (Gao and Shubin, 2012) and insects (Ren et al., 2010), discoveries of feathered dinosaurs in Jianchang County have considerably improved our understanding of the evolution and paleobiology of the Paraves (Xu et al., 2009, 2011; Zheng et al., 2009; Longrich et al., 2012; Godefroit et al., 2013a, 2013b). Fossil deposits in the Tiaojishan Formation in Jianchang County have been dated to ~160 million years ago (Wang et al., 2013), thus, Late Jurassic (Oxfordian) in age (Cohen et al., 2013). These deposits have furnished the most abundant collection of Jurassic paravians in the world. Fossils discovered in these deposits include multiple specimens of *Anchiornis huxleyi, Xiaotingia zhengi, Aurornis xui,* and *Eosinopteryx brevipenna* (Xu et al., 2009, 2011; Hu et al., 2009; Zheng et al., 2009; Godefroit et al., 2013a, 2013b).

The type specimen of *Anchiornis huxleyi* (IVPP V14378) was reported by Xu et al. (2009) from the Tiaojishan Formation in Jianchang County, China. This specimen consists of a semiarticulated postcranial skeleton, missing only parts of the tail and the forelimb. *Anchiornis huxleyi* was briefly described and diagnosed in the original publication, and was assigned to the Avialae based on postcranial similarities with *Archaeopteryx*. A second specimen of *Anchiornis huxleyi*, LPM-B00169, a complete skeleton that includes feathers, was reported by Hu et al. (2009) shortly thereafter. A brief osteological description of the specimen was included in that study, and anatomical details clarified the relationships of *Anchiornis huxleyi,* allowing its reassignment to the Troodontidae (Hu et al., 2009; Turner et al., 2012). Li et al. (2010) reported a third specimen of *Anchiornis huxleyi*, BMNHC PH828. It preserves a semiarticulated skeleton with extensive feathers, yet is missing parts of the tail and several limb and cranial bones. A thorough examination of the microstructure of the plumage in BMNHC PH828 revealed the coloration of *Anchiornis* for the first time in a nonavialan dinosaur species (Li et al., 2010).

Later discoveries of closely related paravians further cloud the phylogenetic position of *Anchiornis huxleyi* as well as other paravians (Xu et al., 2011; Tuner et al., 2012; Agnolín and Novas, 2013; Godefroit et al., 2013a, 2013b; Foth et al., 2014; Brusatte et al., 2014). Yet, despite its

importance and being known from a large number of specimens, the morphology of this taxon has only been described briefly (Xu et al., 2009; Hu et al., 2009; Li et al., 2010; Zheng et al., 2014).

Although only three specimens have been described to date, many nearly complete specimens of *Anchiornis huxleyi* have been recovered from Jianchang County in western Liaoning Province, China (Zheng et al., 2014). A large number of extraordinarily well-preserved specimens afford an excellent opportunity to investigate intraspecific variation, allometric growth, and possible sexual dimorphism in one of the earliest paravians. This study provides full osteological descriptions of four new specimens of *Anchiornis huxleyi.*

Material

Four new specimens of *Anchiornis huxleyi*, PKUP V1068, BMNHC PH804, BMNHC PH822, and BMNHC PH823 (figs. 1–4), from the same locality as the holotype, were recently acquired by Peking University and the Beijing Museum of Natural History. All the new specimens preserve nearly complete and well-exposed cranial and postcranial skeletons.

PKUP V1068 preserves a complete skeleton with some feather imprints scattered around the tail (fig. 1). Unlike many other *Anchiornis huxleyi* specimens, most of whose cranial bones are shattered and dislocated, the skull and the mandibles of PKUP V V1068 are extraordinarily well preserved with most of the bones articulated in life position. The proximal caudal vertebra, the coracoid, and the left pes are not well exposed in this specimen, as they are still buried in matrix or overlapped by other bones. This specimen is one of the largest (based on femoral length) described *Anchiornis* specimens, with an estimated body length of 60 cm (including the unexposed caudal vertebrae) compared to 34 cm of the holotype (table 1).

BMNHC PH804 is a complete and articulated skeleton with feathers preserved on the tail, forelimb, and hindlimb (fig. 2). The skull of BMNHC PH804 is preserved in quasilateral view, and is not as well articulated as in PKUP V1068. The left manus is obscured by the skull and the right metacarpals are not fully prepared. The rest of the skeleton is well exposed. BMNHC PH804 has a body length of about 36 cm, slightly larger than the holotype.

BMNHC PH822 is a complete skeleton. The skull of BMNHC PH822 is exposed in dorsal view (fig. 3). However, several of the cranial bones are shattered and not as well preserved as in PKUP V1068. The postcranium is fully articulated except for the left pes. BMNHC PH822 is about the size of PKUP V1068, based on the skull and femur length, but it has a proportionally longer tail, and thus has a total body length of 62 cm, which is longer than the estimate for PKUP V1068. BMNHC PH822 is preserved with a pair of squamate mandibles in the gastral region and a caudal vertebral column in the thoracic region (fig. 15). We interpret these possibly as the remains of a single lizard ingested before death and burial. The right metatarsus of BMNHC PH822 was possibly reconstructed by local collectors before the acquisition of this specimen by the Beijing Museum of Natural History, and is not included in the description.

BMNHC PH823 is a nearly complete skeleton. The skull is laterally preserved and slightly shattered (fig. 4). Most of the cranial bones are articulated, except for the left mandible, which is broken and fragmented. The pubes of BMNHC PH823 are missing. The cervical vertebrae, the proximal caudal vertebrae and parts of the limb bones were reconstructed by local collectors before the acquisition of the specimen, and thus are not included in the osteological description. BMNHC PH822 has an estimated body length of about 46 cm, based on the positions and lengths of the skull and tail (fig. 4).

This description of *Anchiornis huxleyi* is primarily based on the best-preserved specimen, PKUP V1068. All the other specimens display almost identical morphologies, except where noted.

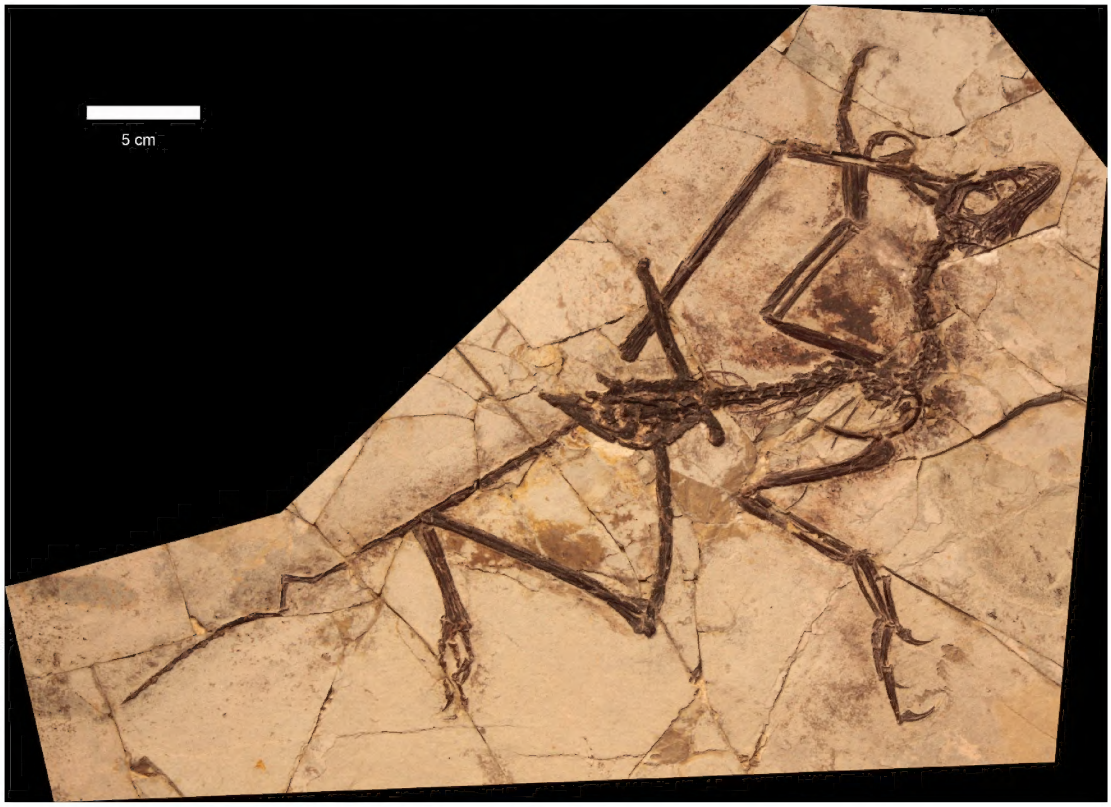

FIGURE 1. Mounted slab of PKUP V1068.

MORPHOLOGICAL DESCRIPTION

Skull and Mandible

The skull of *Anchiornis huxleyi* has a typical basal paravian profile, as in *Archaeopteryx*, *Mei*, *Microraptor,* and *Shanag*. It has a large and round orbit, a large antorbital fossa, and an elongate naris. The snout of *Anchiornis huxleyi* is slightly elongate, but not as much as in *Archaeopteyrx*.

Premaxilla: The right premaxilla of PKUP V1068 is exposed in lateral view. The anterior end of the premaxilla is damaged and the lateral surface of the right premaxilla is eroded, with the premaxillary tooth roots laterally exposed (fig. 5). The main body of the premaxilla (the laterally exposed portion except the nasal process and the subnarial process) lies mostly anterior to the external naris. Only a small posterior portion of the premaxillary body extends ventral to the external naris, as in *Archaeopteryx* (Mayr et al., 2005, 2007), which differs from the condition in troodontids and dromaeosaurids (Makovicky and Norell, 2004; Norell and Makovicky, 2004). The nasal process tapers posterodorsally and is almost three times the length of the premaxillary main body. The nasal process of PKUP V1068 is very similar to that of *Archaeopteryx* (Mayr et al., 2005, 2007), in having an anteroposteriorly expanded base and a premaxillary foramen positioned laterally on the base of the nasal process (fig. 5). As in *Xiaotingia*, *Archaeopteryx*, and *Caudipteryx*, the anterior surface of the nasal process is straight and confluent with the premaxillary body (Ji et al., 1998; Zhou et al., 2000; Mayr et al., 2005; Xu et a., 2011), which is in contrast to other nonavian paravians and *Sapeornis*, where the nasal process is curved and forms an

TABLE 1

Selected Measurements (in mm) of PKUP V1068, BMNHC PH804, BMNHC PH822, and BMNHC PH823.

	PKUP V1068	BMNHC PH804	BMNHC PH822	BMNHC PH823
skull	>61.3	43.5	61.2	56.0
body	~600	~360	~620	~460
scapula left	>37.0	29.1	–	40.1
scapula right	~34.2	29.1	40.8	–
humerus left	>69.5	45.7	61.8	65.2
humerus right	72.2	44.5	64.9	64.5
ulna left	59	39.8	58.9	–
ulna right	58.5	38.8	60.8	–
radius left	52	39.1	>58.0	–
radius right	52.8	38.2	58.9	–
metacarpal I left	12.4	–	–	–
metacarpal II left	32.13	–	–	–
metacarpal III left	>24.5	–	–	–
manual phalanx I-1 left	25	–	–	–
manual phalanx I-2 left	21.8	–	–	–
manual phalanx II-1 left	18.9	11.4	–	–
manual phalanx II-2 left	>21.0	18.1	–	–
manual phalanx II-3 left	>14.5	10.1	20.8	–
manual phalanx III-1 left	–	6.9	–	–
manual phalanx III-2 left	–	6.6	–	–
manual phalanx III-3 left	–	9.5	–	–
manual phalanx III-4 left	–	9	–	–
metacarpal I right	12.7	–	12.6	–
metacarpal II right	35	–	36.2	–
metacarpal III right	29.8	–	32.7	–
manual phalanx I-1 right	26.1	–	29.6	–
manual phalanx I-2 right	>18.0	–	18.6	–
manual phalanx II-1 right	18	–	21.9	–
manual phalanx II-2 right	26.8	–	27.8	–
manual phalanx II-3 right	20.5	–	18.8	–
manual phalanx III-1 right	7.2	–	8.7	–
manual phalanx III-2 right	6.9	–	7.2	–
manual phalanx III-3 right	14.7	–	15.3	–
manual phalanx III-4 right	14	–	13.5	–
ilium left	42.2	–	–	40.9
ilium right	~48.1	25.1	34.8	42.3
pubis left	56.9	39.2	61.4	–

	PKUP V1068	BMNHC PH804	BMNHC PH822	BMNHC PH823
pubis right	55.2	–	–	–
ischium left	–	~19	–	22.1
femur left	88.5	–	–	68.7
femur right	90.5	50.9	70.5	67.8
tibiotarsus left	112	69.5	108.6	95.2
tibiotarsus right	117.7	69.1	108	92.13
metatarsal II left	50.0	39.7	57.8	–
metatarsal III left	51.5	–	58	–
metatarsal IV left	49.1	38.3	56.1	–
pedal phalanx II-1 left	–	8.7	11.2	–
pedal phalanx II-2 left	13	8.3	12.2	–
pedal phalanx II-3 left	–	–	13.3	–
pedal phalanx III-1 left	15	9.8	15.2	–
pedal phalanx III-2 left	10	8	11.2	–
pedal phalanx III-3 left	11.3	7.1	7.8	–
pedal phalanx III-4 left	16.8	7.9	–	–
pedal phalanx IV-1 left	11	7.4	11.6	–
pedal phalanx IV-2 left	9.1	5.2	8.9	–
pedal phalanx IV-3 left	–	5.1	8.4	–
pedal phalanx IV-4 left	–	4.9	7.9	–
pedal phalanx IV-5 left	10.2	6.1	10.8	–
metatarsal I right	–	>6.5	–	–
metatarsal II right	56.2	–	51	49
metatarsal III right	56.4	–	55.2	51.2
metatarsal IV right	55	38.3	54.5	48.5
pedal phalanx I-1 right	–	5.3	–	7.5
pedal phalanx I-2 right	–	4.2	–	–
pedal phalanx II-1 right	13	8.7	–	10.4
pedal phalanx II-2 right	11.5	7.6	–	8.1
pedal phalanx II-3 right	–	9.1	–	13
pedal phalanx III-1 right	15.1	9.7	–	12.8
pedal phalanx III-2 right	–	7.8	–	7.8
pedal phalanx III-3 right	–	7	–	11
pedal phalanx III-4 right	–	7.7	–	13.2
pedal phalanx IV-1 right	11.5	7.4	–	–
pedal phalanx IV-2 right	–	5.2	–	8.8
pedal phalanx IV-3 right	–	5.2	–	7.5
pedal phalanx IV-4 right	–	5.1	–	7.2
pedal phalanx IV-5 right	–	5.0	–	13.4

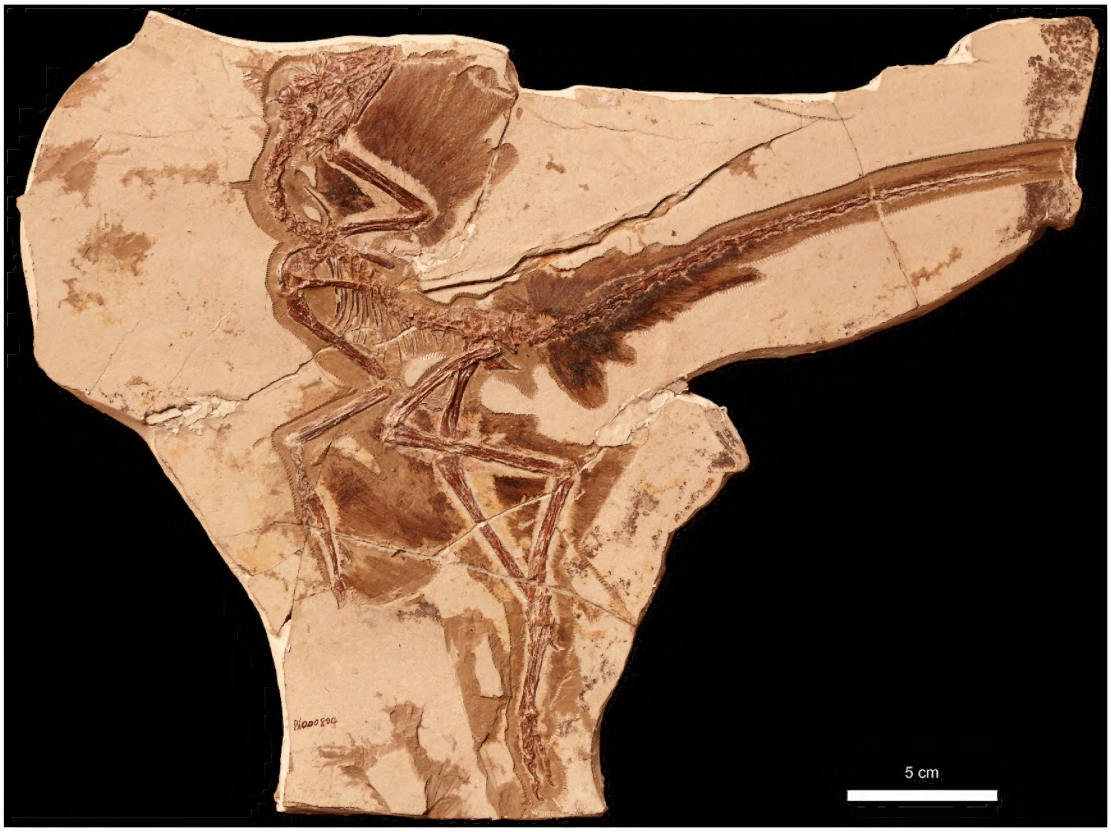

FIGURE 2. Mounted slab of BMNHC PH804.

angle with the anterior surface of the premaxilla body (e.g., Barsbold and Osmólska, 1999; Xu et al., 1999; Zhou and Zhang, 2003). The internarial bar of PKUP V1068 is dorsoventrally flat, as in troodontids and *Archaeopteryx* (Makovicky et al., 2003; Norell et al., 2009; Foth et al., 2014).

The subnarial process of PKUP V1068 is short and slender in lateral view. The subnarial process forms the ventral margin of the naris, a condition seen in several basal paravians, such as *Sinovenator*, *Sinornithosaurus,* and *Archaeopteryx* (Xu et al., 1999, 2000; Mayr et al., 2005). The naris of PKUP V1068 is elongate and subtriangular (fig. 5). The naris is relatively posteriorly positioned, as observed in *Archaeopteryx*, *Jeholornis,* and *Mei* (Zhou and Zhang, 2002; Xu and Norell, 2004; Mayr et al., 2005), as the anterior margin of the naris is posterior to or at the position of the fourth premaxillary tooth. In most dromaeosaurids and described troodontids, the anterior margin of the naris is positioned significantly anterior to the last premaxillary tooth (e.g., Osborn et al., 1924; Xu et al., 2000; Burnham et al., 2000; Ji et al., 2005; Norell et al., 2006; Lü and Brusatte, 2015).

The premaxilla is dislocated in BMNHC PH804 (fig. 6), yet retains an identical morphology as in PKUP V1068. It bears a straight nasal process and the external naris is situated posterior to the fourth premaxillary tooth as in other *Anchiornis* specimens and *Archaeopteryx* (Mayr et al., 2005; Hu et al., 2009). The premaxillae join to form a pointed anterior tip in dorsal view in BMNHC PH822 (fig. 7). The dorsal surface of the internarial bar is flat and the nasal processes insert between the nasals, as in

FIGURE 3. Mounted slab of BMNHC PH822. Dotted line encircles the area that was reconstructed before acquisition of the specimen.

troodontids and *Archaeopteryx* (Mayr et al., 2005; Norell et al., 2009).

Only the third and fourth premaxillary teeth are present on the right premaxilla of PKUP V1068 (fig. 5), and the first two tooth positions are not preserved. The tooth crowns are cone shaped and slightly recurve posteriorly. A distinct constriction is present between the tooth crown and its cylindrical root, as in some other paravians such as *Archaeopteryx* and *Sinovenator* (Xu et al., 2002; Mayr et al., 2005). The third and the fourth teeth are about the same size, and are larger than the first maxillary tooth. The premaxillary teeth are of comparable size to the teeth that lie in the middle of the maxillary toothrow. This condition is also observed in *Archaeopteryx* and troodontids such as *Sinovenator*, yet is unlike dromaeosaurids where the middle maxillary teeth are much larger (Xu, 2002; Mayr et al., 2005; Turner et al., 2012). Four premaxillary teeth are also present in both BMNHC PH804 and BMNHC PH823, and they are positioned anterior to the external naris, as in *Archaeopteryx* (figs. 6, 8). The premaxillary teeth of BMNHC PH804 and BMNHC PH823 are closely packed anteriorly, as in troodontid dinosaurs (Makovicky et al., 2003; Makovicky and Norell, 2004). The last premaxillary tooth is subequal in size to, or slightly larger than, the first three teeth in BMNHC PH804, as in *Archaeopteryx* and troodontids, but unlike dromaeosaurids such as *Microraptor* and *Velociraptor,* whose last premaxillary tooth is relatively small (Barsbold and Osmólska, 1999; Xu, 2002; Mayr et al., 2005).

Maxilla: The maxilla is a large triangular bone covering most of the lateral side of the

FIGURE 4. Mounted slab of BMNHC PH823. Dotted lines encircle the areas that were reconstructed before acquisition of the specimen.

snout and forms the majority of the rostrum. It is laterally exposed in PKUP V1068, BMNHC PH804, and BMNHC PH823.

In PKUP V1068 the rostral ramus of the maxilla extends below the subnarial process of the premaxilla and the external naris, and is slender and subtriangular laterally (fig. 5). The rostral ramus of the maxilla is relatively short in *Anchiornis huxleyi* (fig. 5), less than one-third the length of the antorbital fossa, which is the also the case in other Jianchang paravians, troodontids, and some dromaeosaurids such as *Microraptor* and *Bambiraptor* (Burnham et al., 2000; Xu et al., 2011; Godefroit et al., 2013a, 2013b; Pei et al., 2014). In avialans, derived dromaeosaurids, and some more-basal coelurosaurians, the rostral process of the maxilla is much longer, at more than two-thirds the length of the antorbital fenestra (e.g., Chiappe et al., 1999; Norell and Makovicky, 2004; Mayr et al., 2005, 2007; Turner et al., 2012).

The ascending process of the maxilla rises posterior to the rostral ramus and extends posterodorsally to form the anterodorsal margin of the antorbital fossa. The lateral lamina of the ascending process is extremely reduced, which is

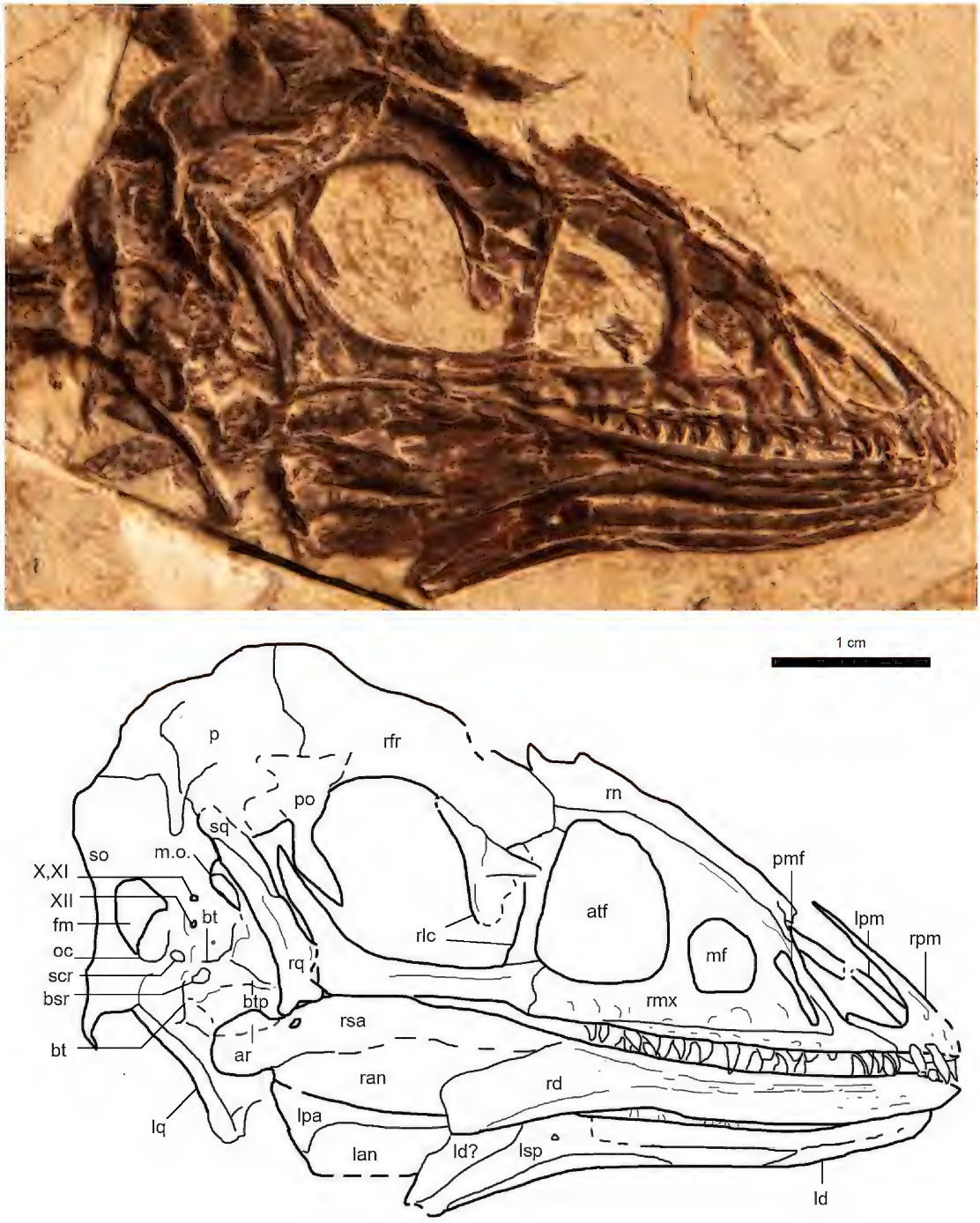

FIGURE 5. Skull of PKUP V1068.

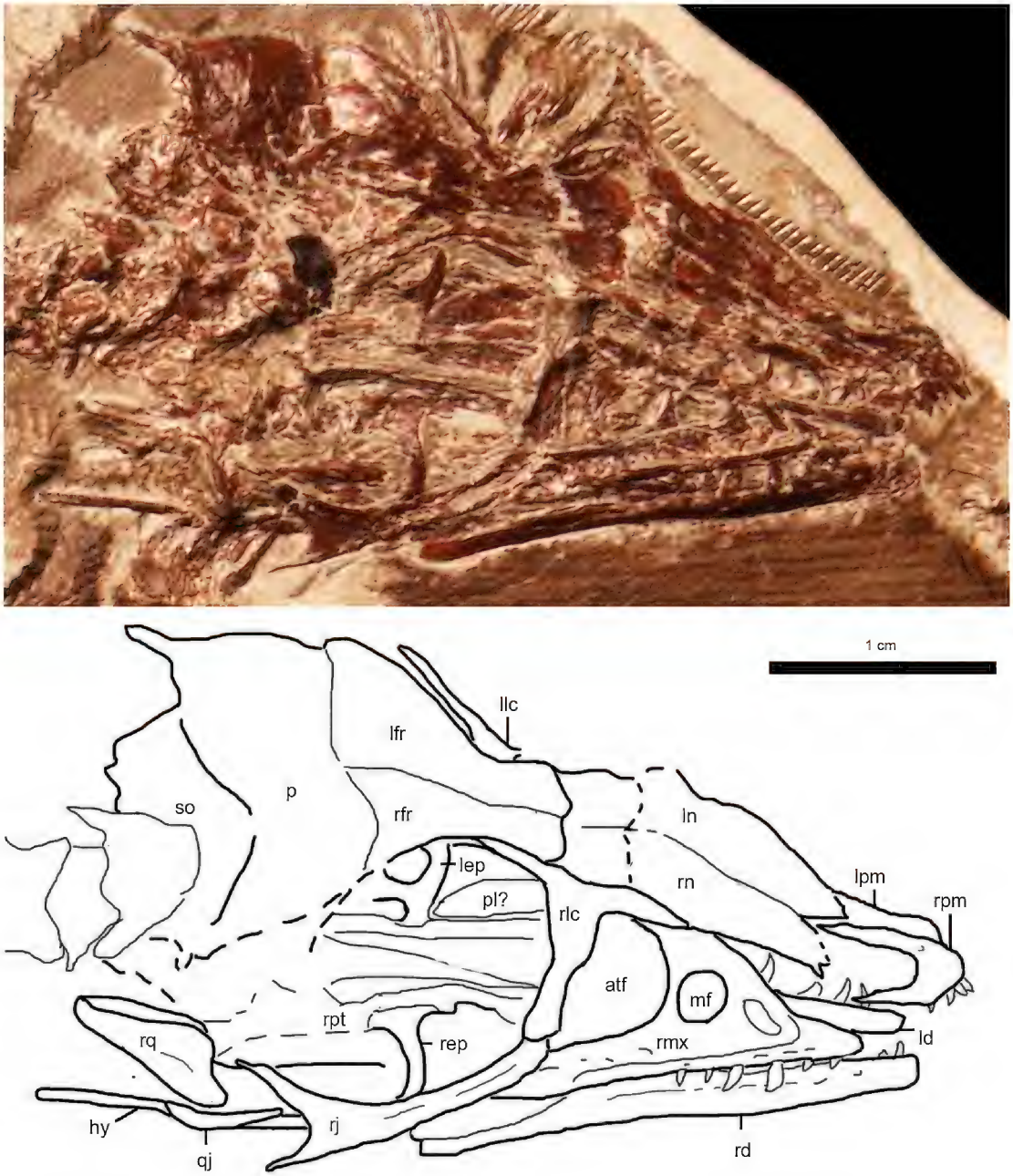

FIGURE 6. Skull of BMNHC PH804.

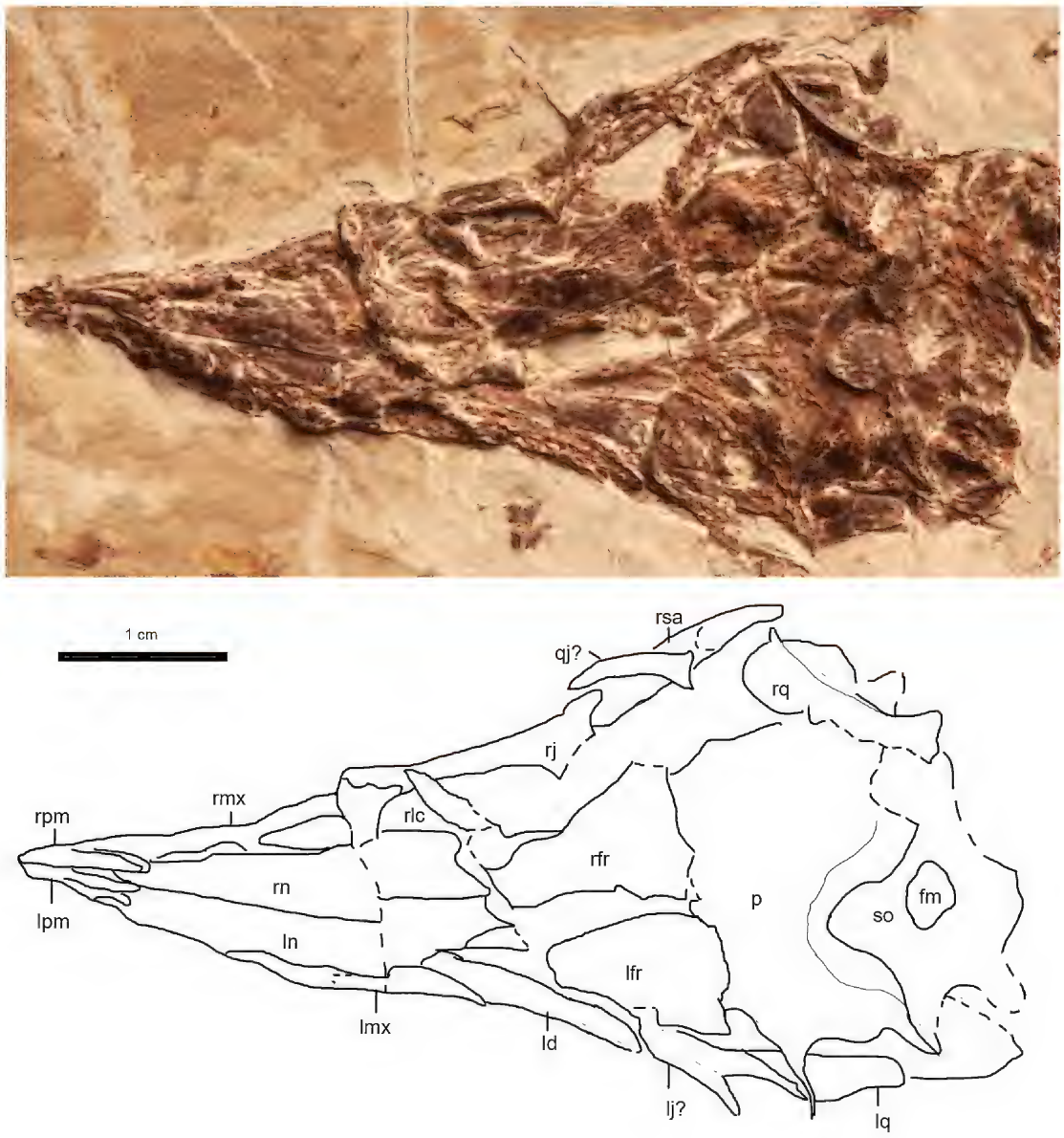

FIGURE 7. Skull of BMNHC PH822.

FIGURE 8. Skull of BMNHC PH823.

similar to the condition in basal troodontids and basal dromaeosaurids, such as *Sinovenator* and *Microraptor*, as well as *Archaeopteryx* (Xu et al., 2000, 2002; Mayr et al., 2005, 2007; Pei et al., 2014). In derived troodontids and dromaeosaurids, the lateral lamina of the ascending process is broad (Osborn et al., 1924; Norell et al., 2006; Xu et al., 2010; Tsuihiji et al., 2014).

The horizontal posterior ramus continues from the rostral ramus, and tapers posteriorly in PKUP V1068 (fig. 5). The posterior ramus is slightly dorsoventrally shallower than the rostral ramus, unlike *Archaeopteryx*, *Mei,* and *Sinovenator*, in which the posterior ramus is almost as deep as the rostral ramus (Xu et al., 2002; Xu and Norell, 2004; Wellnhofer, 2009). A horizontal ridge is developed above the toothrow on the posterior ramus, as seen in many coelurosaurian dinosaurs. It forms a well-defined ventral margin of the large antorbital fossa. A series of neurovascular foramina occurs along the posterior ramus and dorsal to the toothrow. The posterior end of the posterior ramus tapers in PKUP V1068, as in *Archaeopteryx* and dromaeosaurids (Mayr et al., 2007; Turner et al., 2012). This is different from troodontids, where the posterior ramus has nearly parallel dorsal and ventral edges (e.g., Xu et al., 2002; Makovicky et al., 2003; Norell et al., 2009; Lü et al., 2010).

The antorbital fossa is located dorsal to the posterior ramus. It is anteriorly bounded by the ascending process of the maxilla. The anteroventral corner of the antorbital fossa is almost rectangular, resembling that of *Sinovenator*, but different from *Archaeopteryx* and *Microraptor*, in which the anteroventral corner of the antorbital fossa is rounded (Xu et al., 2002; Mayr et al., 2005, 2007; Pei et al., 2014). In contrast to deinonychosaurians, in which the lacrimal and the maxilla form the dorsal border of the antorbital fossa, the antorbital fossa of *Anchiornis* is bounded dorsally by the nasal and the lacrimal as in *Archaeopteryx* (Mayr et al., 2005, 2007).

A slitlike promaxillary fenestra is located at the anteriormost part within the antorbital fossa, which is a primitive condition in paravians, such as in *Microraptor*, *Sinovenator,* and *Archaeopteryx* (Xu, 2002; Mayr et al., 2007; Rauhut, 2014; Pei et al., 2014). The promaxillary fenestra is elongate in PKUP V1068, and its long axis inclines posterodorsally. The long axis of the promaxillary fenestra is as long as the longest diameter of the maxillary fenestra (fig. 5). The ventral margin of the premaxilla fenestra is in a more ventral position compared to that of the maxillary fenestra and the antorbital fenestra, which is similar to the condition in *Microraptor*, but different from that in *Archaeopteryx* and troodontids (Xu et al., 2002, Mayr et al., 2007; Pei et al., 2014). Unlike dromaeosaurids, the space between the maxillary fenestra and the promaxillary fenestra is anteroposteriorly short in PKUP V1068, which is similar to troodontids and *Archaeopteryx* (Xu et al., 2002; Mayr et al., 2007; Rauhut, 2014; Pei et al., 2014).

A round maxillary fenestra lies posterodorsal to the promaxillary fenestra in PKUP V1068. The maxillary fenestra is relatively large, as in troodontids, *Aurornis*, and *Archaeopteryx*, but different from the condition in dromaeosaurids, in which the maxillary fenestra is reduced in size (Wellnhofer, 1974; Xu et al., 2002; Mayr et al., 2005, 2007; Norell and Makovicky, 2004; Godefroit, 2013b). The size of the maxillary fenestra is about one-fourth that of the antorbital fenestra in area, not as large as in *Jinfengopteryx*, but similar to *Sinovenator* and *Archaeopteryx* (Wellnhofer, 1974; Xu et al., 2002; Mayr et al., 2005, 2007; Ji et al., 2005). The ventral margin of the maxillary fenestra is at the same level as the ventral margin of the antorbital fenestra, as in troodontids and *Archaeopteryx*, but not dorsally displaced as in dromaeosaurids (Makovicky and Norell, 2004; Norell and Makovicky, 2004; Mayr et al., 2005, 2007; Turner et al., 2012).

An interfenestral bar separates the maxillary fenestra from the antorbital fenestra in PKUP V1068. The ventral base of the interfenestral bar is anteroposteriorly expanded. The upper portion of the interfenestral bar leans posteriorly and contacts the dorsal ramus of the maxilla. Whether an interfenestral canal is present as in

FIGURE 9. Dentition of PKUP V1068. Scale bar = 5 mm.

Byronosaurus (Makovicky et al., 2003) cannot be confirmed in this specimen.

The antorbital fenestra is a large opening positioned posterior to the interfenestral bar. It is pear shaped with a horizontal ventral margin and a slightly posteriorly sloping dorsal margin. The ventral margin of the antorbital fenestra is level with that of the maxillary fenestra and the orbit, but higher than those of the premaxillary fenestra and the external naris. The dorsal margin of the antorbital fenestra is shorter than the ventral margin, as observed in many basal paravians (e.g., Xu et al., 2011; Rauhut, 2014).

The maxilla is shattered in BMNHC PH804 and only vague outlines can be observed (fig. 6). As in PKUP V1068, the rostral ramus is short and semitriangular, and the ventral ramus has a tapering posterior end. An elongate promaxillary fenestra is located posterodorsal to the rostral ramus, within the antorbital fossa, and more ventrally displaced than the maxillary fenestra. A round maxillary fenestra is posterior to the promaxillary fenestra. The antorbital fenestra is large, with a diameter about twice that of the maxillary fenestra. The interfenestral bar between the antorbital fenestra and the maxillary fenestra is anteriorly inclined, which differs from other specimens in which the bar is more vertical, but this is probably a preservational artifact (fig. 6). The maxilla of BMNHC 823 is too shattered to provide additional information.

In PKUP V1068, 14 maxillary teeth are preserved and exposed on the right side (fig. 9). This number is similar to dromaeosaurids, *Archaeopteryx*, and *Jinfengopteryx*, but is less than in other troodontids (Makovicky and Norell, 2004; Norell and Makovicky, 2004; Ji et al., 2005; Mayr et al., 2005, 2007). Maxillary teeth are more curved than the premaxillary teeth. The anteriormost maxillary teeth are smaller than the premaxillary teeth, and the first two maxillary teeth are more slender than the others (fig. 9). The anterior three teeth are closely packed, and the middle and posterior teeth are loosely packed, as in *Sinovenator* and *Mei* (Xu et al., 2002; Xu and Norell, 2004), in contrast to the condition in *Jinfengopteryx* and derived troodontids (e.g., *Byronosaurus* and *Zanabazar*) (Makovicky et al., 2003; Ji et al., 2005; Norell et al., 2009), in which all the maxillary teeth are closely packed. Unlike many troodontids (e.g., *Sinovenator*, *Sinornithoides*, *Troodon*, and *Zanabazar*) and dromaeosaurids, no serrations are present on the maxillary teeth, which is the primitive condition in paravians (Elzanowski and Wellnhofer, 1996; Makovicky et al., 2003; Xu and Norell, 2004). The posterior teeth are reduced in size. The last six exposed teeth display a constriction between the root and the crown, as in many paravian taxa (e.g., Xu et al., 2000; Makovicky et al., 2003; Wellnhofer, 2009; Pei et al., 2014) except for some dromaeosaurids (e.g., Burnham et al., 2000; Turner et al., 2007).

Nasal: The right nasal is exposed in quasilateral view in PKUP V1068 (fig. 5). The nasals are elongate. Anteriorly, the nasal forms the posterodorsal border of the external naris. Laterally, the nasal sutures with the maxilla along a straight line, as observed in BMNHC PH804, but does not contribute to the dorsal margin of the antorbital fossa (fig. 6), as it does in *Archaeopteryx*, dromaeosaurids, and troodontids (e.g., Burnham et al., 2000; Makovicky et al., 2003; Rauhut, 2014; Pei et al., 2014; Tsuihiji et al., 2014).

The nasals are well exposed in dorsal view in BMNHC PH822 (fig. 7). They are paired, with a straight midline suture between the two elements. The nasals are elongate, with a length more than three times the width. Anteriorly, the nasal processes of the premaxillae insert between the nasals, as in other paravians. Posteriorly, the nasals suture the frontal with a W-shaped suture typical of paravians, but unlike the condition in *Zanabazar* and *Gobivenator*, where the nasals wedge between the frontals (Norell et al., 2009; Tsuihiji et al., 2014). The nasals extend posterior to the anterior margin of the orbit, a basal paravian condition also observed in *Jinfengopteryx* and *Archaeopteryx* (Mayr et al., 2005; Ji and Ji, 2007). This differs from some dromaeosaurids and troodontids, such as *Tsaagan* and *Mei*, where the suture is anterior to the orbit (Xu and Norell, 2004; Norell et al., 2006). The posterior part of the nasal is broken transversely dorsal to the lacrimal in BMNHC PH822 and BMNHC PH804 (figs. 6, 7). A similar breakage is present in some *Archaeopteryx* specimens, notably in the Thermopolis specimen (Rauhut, 2014), and may reflect the fragility of the nasal bones in basal paravians.

Frontal: The frontals are paired and unfused. The right frontal is dislocated from its original position in PKUP V1068 (fig. 5). Anteriorly, the frontals contact the nasals and the lacrimals. The suture with the nasal is W-shaped, as observed in BMNHC PH804, BMNHC PH822, *Mei,* and *Archaeopteryx* (figs. 6, 7) (Xu and Norell, 2004; Rauhut, 2014). A notch is developed on the lateral edge of the frontal anteriorly, to receive the posterior process of the lacrimal (fig. 5), as in many deinonychosaurians (Norell and Makovicky et al., 2004; Makovicky and Norell, 2004). The frontals contact along a straight midline suture. A thick supraorbital rim is developed to border the orbit in PKUP V1068, which is common in paravians (e.g., *Microraptor*, *Mei,* and *Archaeopteryx*). Posteriorly, the frontal mediolaterally expands in dorsal view and bears a W-shaped suture at its contact with the parietal, as observed in PKUP V1068 and BMNHC PH004. The suture with the parietal appears straighter in BMNHC PH822 and BMNHC PH823 than in other specimens of this taxon (figs. 5–8).

Lacrimal: The right lacrimal is broken into two pieces in PKUP V1068 (fig. 5). The anterior and posterior processes are broken away from the ventral process and attached to the displaced frontal. The remaining parts of the anterior and posterior processes are subequal in length, a primitive condition of paravians, but in contrast to the longer anterior process of derived troodontids (Makovicky et al., 2003; Norell et al., 2009; Tsuihiji et al., 2014). Unlike troodontids and dromaeosaurids, the lacrimal of PKUP V1068 lacks a recess ventral to the anterior process (e.g., Burnham et al., 2000; Makovicky et al., 2003; Xu et al., 2010; Tsuihiji et al., 2014). The lacrimal does not bear an expanded supraorbital ridge anterodorsal to the orbit, which is different than in most troodontids (Makovicky et al., 2003; Xu and Norell, 2004; Norell et al., 2009; Tsuihiji et al., 2014). The ventral process appears to suture the suborbital process of the jugal along a robust contact. The ventral process is straight and slightly inclined along an anterodorsal-posteroventral axis. The ventral process of the lacrimal is bandlike, with almost parallel anterior and posterior edges. It bears a distinct posterolateral ridge, and borders the orbit anteriorly.

The lacrimal of BMNHC PH804 is completely preserved (fig. 6). The anterior and posterior processes of the lacrimal are slender and subequal in length, as in *Microraptor* and basal troodontids like *Jinfengopteryx* (Ji et al., 2005; Pei et al., 2014). The anterior process covers the entire dorsal margin of the antorbital fenestra, as in other paravians (Xu et al., 2002; Mayr et al., 2007; Turner et al., 2012). The posterior process contacts the frontal laterally and forms the anterodorsal margin of the orbit (fig. 6). Unlike in derived troodontids and dromaeosaurids (e.g., Barsbold and Osmólska, 1999; Xu and Norell, 2004; Pei et al., 2014; Tsuihiji et al., 2014), the posterior process is much more slender compared to the ventral process of the lacrimal. BMNHC PH822 is similar with elongate and slender anterior and posterior processes (fig. 7). As in BMNHC PH804, the anterior process

forms the dorsal margin of the antorbital fenestra and the posterior process forms the anterodorsal margin of the orbit. As both the anterior and posterior processes are extremely slender and fragile in *Anchiornis*, they are easily damaged during preservation, collection, or preparation. In BMNHC PH823, the anterior and ventral processes of the lacrimal are broken apart, and the posterior process is missing (fig. 8).

Jugal: The right jugal is well exposed in PKUP V1068, but the posterior end of the bone is damaged (fig. 5). The suborbital process of the jugal is horizontally oriented, contacting the posterior end of the maxilla. It forms the ventral border of the round orbit and contributes to the posteroventral corner of the antorbital fossa, which is a primitive condition in paravians (Xu, 2002; Xu and Norell, 2004; Mayr et al., 2005, 2007). The suborbital process of the jugal is straight, with a horizontal groove on the lateral surface as seen in many paravians such as *Microraptor* and *Sinovenator* (Xu, 2002; Xu et al., 2002; Pei et al., 2014). A shallow concavity is developed at the posterior end of the groove in lateral view. The postorbital process of the jugal tapers posterodorsally, and it is shorter than the suborbital process. The jugal of BMNHC PH804 and BMNHC PH823 is identical to that of PKUP V1068 (figs. 6, 8). It is laterally grooved on the suborbital process and bears a slender postorbital process, which forms ~135° angle with the suborbital process, typical of primitive paravians. Medially, the hooked jugal process of the ectopterygoid contacts the jugal at the midpoint of the suborbital bar. The quadratojugal process of the jugal is observed in BMNHC PH804 and BMNHC PH823 (figs. 6, 8). The quadratojugal process is slender and short, and confluent with the ventral margin of the suborbital process, as in *Xiaotingia* and *Microraptor*, but not as well developed as in anatomically derived dromaeosaurids such as *Tsaagan* (Xu, 2002; Norell et al., 2006; Xu et al., 2011). In contrast to *Archaeopteryx* (Foth et al., 2014; Rauhut, 2014) and *Microraptor* (Pei et al., 2014), but as in other theropods, there is a rounded margin between the quadratojugal process and the postorbital process, showing no incision. Unlike many deinonychosaurians (e.g., Norell et al., 2006; Tsuihiji et al., 2014), the quadratojugal process of the jugal of BMNHC PH804 is rodlike and lacks a notch.

Postorbital: The right postorbital is dislocated in PKUP V1068, and its dorsal portion is missing. Only the ventral process is recognizable (fig. 5). The slender ventral process is mediolaterally flattened, and about the same size as the postorbital process of the jugal. As other paravians, the postorbital probably has a posterodorsally inclined suture with the jugal. The postorbital and the jugal form a closed postorbital bar as in most theropods including *Archaeopteryx* (Rauhut, 2014). An unidentified bone ventral to the parietal in BMNHC PH823 possibly represents the jugal process of the postorbital (fig. 8); it is slender as in PKUP V1068.

Quadratojugal: No trace of the quadratojugal is observed in IVPP V1068. A possible quadratojugal is observed in BMNHC PH804, BMNHC PH822, and BMNHC 823 (figs. 6–8). The quadratojugal is reduced in size and L-shaped, without a horizontal posterior process, as in *Archaeopteryx*, troodontids, and oviraptorosaurs, but unlike the reversed T-shaped quadratojugal in dromaeosaurids (Norell and Makovicky, 2004; Balanoff and Norell, 2012; Turner et al., 2012; Pei et al., 2014; Tsuihiji et al., 2014).

Quadrate: The right quadrate of PKUP V1068 is exposed in lateral view and the left quadrate is exposed in posteromedial view (fig. 5). The anterior edge of the right quadrate is damaged. The quadrate inclines anteroventrally, as is typical of most troodontids and *Archaeopteryx*, but different from the vertical quadrate of *Mei* and dromaeosaurids such as *Tsaagan*, *Velociraptor,* and *Microraptor* (Barsbold and Osmólska, 1999; Xu and Norell, 2004; Norell et al., 2006; Norell et al., 2009; Rauhut, 2014; Pei et al., 2014). Dorsally, the quadrate contacts the ventral process of the squamosal along a posterodorsally inclined suture, as in dromaeosaurids (Norell and Makovicky, 2004). A distinct lateral groove is developed on the middle and lower

portion of the quadrate shaft. The anterior edge of the quadrate blade laterally flares anterior to the groove, to form a low ridge, possibly representing the anterior flange in dromaeosaurid dinosaurs. The quadrate is notched below the anterior flange, as in *Archaeopteryx*, *Xiaotingia*, and dromaeosaurids (fig. 5) (Wellnhofer, 1974; Xu et al., 2011; Turner et al., 2012). The posterior edge of the quadrate blade is thickened, as observed on the left element. The pterygoid wing is wider than the jugal wing, as can be determined from the exposed ventral edge of the left quadrate (fig. 5). The quadrate foot is straight and oriented vertically. It is tongue shaped and has a bicondylar connection with the mandible as is typical of paravians.

The right quadrate is exposed in lateral view in BMNHC PH804 and BMNHC PH822 (figs. 6, 7). It is triangular in outline and laterally grooved. It bears an anterior flange, as in dromaeosaurids (Norell and Makovicky, 2004; Turner et al., 2012). An anterior notch is developed ventral to the anterior flange as in PKUP V1068. Medially, the quadrate of BMNHC PH804 appears to contact with an unidentified element that is possibly interpreted as the prequadrate wing of the pterygoid (fig. 6).

Squamosal: A fractured bone piece anterodorsal to the quadrate possibly represents the ventral process of the squamosal in PKUP V1068 (fig. 5). It sutures the quadrate blade and forms the posterodorsal margin of the upper temporal fenestra. The ventral process of the squamosal reaches the midpoint of the quadrate shaft and contacts the anterior flange, as in dromaeosaurids, but differing from the condition in troodontids, where the ventral process of the squamosal is relatively short. The ventral process of the squamosal probably does not contact the quadratojugal as in *Archaeopteryx* and troodontids, judging from its length and the reduced size of the quadratojugal in *Anchiornis huxleyi*, which is different from dromaeosaurids (Norell and Makovicky, 2004).

Parietal: The parietal is articulated with the frontals in PKUP V1068 (fig. 5). The parietal is vaulted and is slightly anteroposteriorly shorter than the frontal. The parietals are fused in PKUP V1068, BMNHC PH804, BMNHC PH822, and BMNHC PH823 (although the parietal is shattered in BMNHC PH822), as in deinonychosaurians (even small-bodied taxa such as *Mei*), but differing from the paired parietals in *Archaeopteryx* (Xu and Norell, 2004; Mayr et al., 2005, Turner et al., 2012). A weak sagittal crest is present along the midline of the fused parietals. The parietal-squamosal nuchal wing is prominent and tapers posterolaterally in dorsal view in BMNHC PH804 and BMNHC PH823 (figs. 6, 8).

Palatal elements: Some palatal elements are exposed through the orbit of BMNHC PH804 (fig. 6). Both ectopterygoids are preserved in their original position in this specimen. The ectopterygoid has a concave anterior margin, and a jugal process that curves posteriorly and joins the jugal at the medial side of the suborbital bar, as in other paravians such as *Archaeopteryx*, *Dromaeosaurus*, and *Saurornithoides* (Witmer, 1997; Mayr et al., 2007; Norell et al., 2009). Medially, the ectopterygoid contacts the pterygoid. The pterygoid is elongate, and its prequadrate wing contacts the quadrate posteriorly (fig. 6). The posterior process of the palatine is visible through the orbit, anterior to the jugal process of the ectopterygoid (fig. 6). The posterior process of the palatine is elongate, as is typical of paravians (Witmer, 1997; Mayr et al., 2007; Tsuihiji et al., 2014).

Braincase: The supraoccipital is exposed in posterior view in PKUP V1068 and BMNHC PH822 (figs. 5, 7). It is triangular and bears a prominent medial nuchal crest. The paroccipital process extends lateroventrally in PKUP V1068 and BMNHC PH822, as is typical of basal paravians. The ventral edge of the paroccipital process is thickened.

The foramen magnum of PKUP V1068 and BMNHC PH822 is dorsoventrally shorter than wide (figs. 5, 7), which differs from the condition in anatomically derived troodontids, but resembles *Archaeopteryx*, many higher avialans, alva-

rezsaurids, and dromaeosaurids (Barsbold and Osmólska, 1999; Alanso et al., 2004; Turner et al., 2007; Perle et al., 1999). In PKUP V1068 and BMNHC PH822, the foramen magnum is upside down heart shaped, much like the profile in *Archaeopteryx* and modern avians (Alanso et al., 2004). The occipital condyle of PKUP V1068 is slightly smaller than the foramen magnum. The condyle is shallow and slightly U-shaped in posterior view, and a constriction is developed at its base. Lateral to the occipital condyle and posterior to the right paroccipital wing, a small foramen represents the opening of cranial nerve XII, and a larger opening lateral to it probably represents the opening of cranial nerve X and/or XI, as is observed in other paravians such as *Byronosaurus*, *Zanabazar*, *Velociraptor*, *Tsaagan,* and *Archaeopteryx* (fig. 5) (Makovicky et al., 2003; Norell et al., 2004, 2006, 2009; Alanso et al., 2004).

The ventral surface of the posterior portion of the braincase is exposed in PKUP V1068. An oval subcondylar recess is developed anterior to the occipital condyle and within the basioccipital ventrally (fig. 5). This is a novel feature that has not been reported in other paravians. The basal tubera of PKUP V1068 are weakly developed compared with those in dromaeosaurids, in which the basal tubera are more distinct and ridgelike. The basisphenoid recess is present anterior to the basal tubera (fig. 5), which is a primitive feature in coelurosaurians, and is observed in dromaeosaurids and *Archaeopteryx* but not troodontids (Xu, 2002; Norell et al., 2006; Turner et al., 2012; Rauhut, 2014). The basisphenoid recess of PKUP V1068 appears heart shaped in ventral view, and likely resembles the triple openings in the subsphenoid recess of dromaeosaurids such as *Tsaagan* (Norell et al., 2006). A rodlike bony element anterolateral to the basisphenoid recess contacts the quadrate medially and may represent the basipterygoid process (fig. 5). It is anteriorly projected, as is typical in basal paravians (Xu et al., 2002; Norell et al., 2006; Turner et al., 2012).

A pair of ridges extends anterolaterally from the basal tubera in PKUP V1068 (fig. 5), as in the unnamed troodontid IGM 100/1126. These ridges define a pair of subotic areas ventral to the ventral margin of the middle-ear opening. The subotic area on each side bears a shallow concavity. This subotic area may be homologous to the subotic recess of anatomically derived troodontid dinosaurs (Makovicky et al., 2003; Norell et al., 2009). The middle-ear opening is located anterior to the base of the paroccipital process (fig. 5). It appears elongate as in *Troodon* (Currie and Zhao, 1993), but the detailed otic structure cannot be determined in the available specimens.

Dentary: Both dentaries are completely preserved in PKUP V1068 (fig. 5). The right dentary is exposed in lateral view, partially overlapping the medially exposed left dentary. The dorsal edge of the anterior tip of the dentary slightly turns downward, which is a primitive condition in maniraptorans, and also is observed in many other paravians, such as *Microraptor*, *Archaeopteryx, Sinovenator*, and *Bambiraptor* (Burnham et al., 2000; Hwang et al., 2002; Xu et al., 2002; Mayr et al., 2005, 2007). The dorsal edge of the dentary of PKUP V1068 is concave, while the ventral edge is convex, which is also observed in troodontids such as *Byronosaurus* (Makovicky et al., 2003). A deep groove, penetrated with neurovascular foramina, extends along the lateral side of the dentary, which was proposed to be a diagnostic feature for all troodontid dinosaurs (Makovicky et al., 2003), but is also present in other paravians such as *Buitreraptor* and *Archaeopteryx* (Wellnhofer, 1974; Makovicky et al., 2005). This dentary groove opens posteriorly between a distinct posterodorsal ridge and a posteroventral ridge in *Anchiornis,* as in *Xiaotingia* and *Aurornis* (Xu et al., 2011; Godefroit et al., 2013b). A sheetlike posteroventral process of the dentary lies posterior to the caudal opening of the lateral groove and covers the anterior portions of the angular and surangular (fig. 5). This feature in *Anchiornis* is similar to *Eosinopteryx* (Godefroit et al., 2013a), but differs from other paravians (e.g. Osborn et al., 1924; Xu, 2002; Xu and Norell, 2004; Norell et

al., 2006; Wellnhofer, 2009; Pei et al., 2014), in which the posteroventral process of the dentary tapers. Medially, the dentary bears a deep Meckelian groove (fig. 5).

A partial right dentary is exposed in BMNHC PH804 (fig. 6). It is grooved on the lateral side, and with two rows of foramina developed laterally, as in *Microraptor* (Pei et al., 2014). The dentary is slightly convex on the ventral edge. BMNHC PH804 also bears a sheetlike posteroventral process, as in PKUP V1068, *Eosinopteryx* and *Aurornis* (fig. 6) (Godefroit et al., 2013a, 2013b). In BMNHC PH823, both dentaries are exposed in lateral view (fig. 8). The right dentary is damaged at the posterior end of the lateral groove. The large opening in the right dentary of BMNHC PH823 is a preservational artifact and is not observed on the left dentary (fig. 8). The posteroventral process is also sheetlike in BMNHC PH823.

At least 12 teeth are preserved on the right dentary of PKUP V1068 (fig. 9), and 10 dentary teeth are preserved on the left dentary of BMNHC PH823 (fig. 8). However, 16 dentary tooth positions are estimated to have been present on each dentary, based on the length of the toothrow. The dentary teeth are not serrated, as in other basal paravians and some troodontids, such as *Archaeopteryx*, *Jinfengopteryx*, *Byronosaurus,* and *Gobivenator* (Makovicky et al., 2003; Ji et al., 2005; Mayr et al., 2007; Tsuihiji et al., 2014). The dentary teeth of *Anchiornis* have a similar shape and size as the corresponding maxillary teeth, with constrictions between the roots and tooth crowns, as in other maniraptorans. As in *Archaeopteryx,* but differing from troodontids, interdental plates are present along the medial side of the dentary toothrow in PKUP V1068 (Xu, 2002; Averianov and Sues, 2007; Foth et al., 2014).

Splenial: The splenial is exposed medially on the left mandible of PKUP V1068 (fig. 5). The splenial is a broad sheet that covers the middle part of the medial side of the mandible. As in *Archaeopteryx* and other coelurosaurs, the splenial has a roughly triangular medial exposure (Elżanowski, 2001). The splenial tapers both anteriorly and posteriorly. The broad middle portion of the splenial is penetrated by a small opening in PKUP V1068, which is not observed in other paravians. Unlike deinonychosaurians, the splenial of *Anchiornis* is restricted to the medial side of the mandible, without any lateral exposure (Currie, 1995; Makovicky et al., 2003; Turner et al., 2012).

Angular: The right angular of in PKUP V1068 is laterally exposed and the left angular is exposed medially (fig. 5). Laterally, the right angular forms the posteroventral margin of the mandible. The anterior part of the angular is laterally covered by the sheetlike posteroventral process of the dentary. Laterally, the angular sutures the surangular extensively, and the external mandibular fenestra is not visible in lateral view. The external mandibular fenestra is also absent in basal avialans such as *Aurornis*, *Eosinopteryx*, *Archaeopteryx*, *Jeholornis,* and *Sapeornis* (Zhou and Zhang, 2003; Mayr et al., 2005, 2007; Godefroit et al., 2013a, 2013b), in contrast to the distinct external mandibular fenestra of most other coelurosaurians (except for some compsognathids and *Ornitholestes*), especially deinonychosaurians. Medially, the angular sutures to the prearticular.

Surangular: The right surangular of PKUP V1068 is exposed in lateral view (fig. 5). It forms the upper portion of the posterior part of the mandible in lateral view. It is dorsoventrally broad. A prominent lateral ridge is present on the dorsal edge of the right mandible, which is typical of many paravians. A small surangular foreman lies near the mandible joint on the surangular in PKUP V1068 and BMNHC PH823. A similar foramen is also present in the referred specimen LPM-B00169 and in *Xiaotingia*, but the surangular foramen in *Xiaotingia* is proportionally larger (Hu et al., 2009; Xu et al., 2011). The surangular and the angular are dorsoventrally expanded, making the mandible much deeper posteriorly than anteriorly, as in *Xiaotingia*, *Aurornis,* and *Eosinopteryx* (Xu et al., 2011; Godefroit et al., 2013a, 2013b).

FIGURE 10. Cervical series of PKUP V1068.

Prearticular: The prearticular is partially exposed on the left mandible of PKUP V1068 (fig. 5). It continues from the retroarticular process, and sutures the angular ventrally. The prearticular curves anterodorsally, as in other paravians such as *Tsaagan* (Norell et al., 2006).

Articular: The articular forms the bottom of the mandibular joint in PKUP V1068 (fig. 5). It contributes to a short retroarticular process, and a prominence is present posterior to the mandibular joint, as in other paravians. As in *Archaeopteryx*, this prominence is mostly medially expanded and slightly flares dorsally, but is unlike the distinctly vertical prominence that is characteristic of dromaeosaurids (Norell and Makovicky, 2004; Wellnhofer, 2009).

Postcranium

Cervical vertebrae: Ten cervical vertebrae are preserved in PKUP V1068 (fig. 10), as is typical of coelurosaurian dinosaurs. They are exposed in dorsal view, and are closely associated with each other; the first three cervical vertebrae are heavily eroded on the dorsal surface. The centra of the axis and the 3rd vertebra are shorter than those of the 4th to 7th cervical vertebrae. The prezygapophyses extend anterolaterally and the postzygapophyses extend posterolaterally, giving the neural arch an X-shaped pattern in dorsal view, which is a common feature shared with paravians (Wellnhofer, 1974; Norell et al., 2001). On the 4th to 6th cervical vertebrae, a small

ridge on the postzygapophyses may represent the epipophysis (fig. 10). A lateral lamina lies posterior to the prezygapophyses, posteriorly from the 4th cervical vertebrae, overhanging laterally to the neural arch, which is observed in many theropods. The centra reach maximum at the 6th and 7th cervical vertebrae, which is also the case in other paravians, such as *Archaeopteryx*, *Mei,* and *Microraptor* (Xu and Norell, 2004; Wellnhofer, 2009; Pei et al., 2014). The centra of the 8th to 10th cervical vertebrae are shortened (fig. 10). The postzygapophyses of the 7th to 10th cervical vertebrae are more laterally projecting, as in *Xiaotingia* and *Archaeopteryx* (Xu et al., 2011).

Ten cervical vertebrae are preserved In BMNHC PH804 and exposed in quasilateral view (fig. 11). The anterior cervical vertebrae bear weak neural spines and, as in PKUP V1068, the neural arch is X-shaped in dorsal view. Starting from the 6th vertebra, the postzygapophyses are more laterally spread than are the anterior ones. The centra are ventrally concave, as observed in the 5th to 9th cervical vertebra.

Ten cervical vertebrae are preserved In BMNHC PH822 (fig. 12). The centra are slightly laterally concave in dorsal view. The zygapophyses are prominent, giving the neural arches an X-shape in dorsal view, as in PKUP V1068 and BMNHC PH804. The anterior cervical vertebrae of BMNHC PH822 have flat ventral surfaces. The centra are elongate in the anterior and middle cervical vertebra, but shorter in the 8th, 9th, and 10th cervical vertebrae. As in PKUP V1068 and BMNHC PH804, the postzygapophyses are laterally directed. The cervical ribs are slender and longer than the centra in the 3rd to the 7th cervical vertebrae, and they become shortened posteriorly. The cervical rib on the 7th centrum bears a groove dorsally along the shaft.

Dorsal vertebrae: Twelve dorsal vertebrae are present in PKUP V1068 (fig. 13). The anterior dorsal vertebrae are closely packed, and the centra are relatively short, like those of the posterior cervical vertebrae. Most of the dorsal vertebrae are laterally exposed, except the anteriormost and the last one. Anterior dorsal vertebrae bear short neural spines. The postzygapophyses extend posterolaterally from the neural arch, as in other paravians, and they are more laterally spread than the prezygapophyses. The transverse processes are slender on anterior and middle dorsal vertebrae of PKUP V1068. In the posterior dorsal vertebrae, the postzygapophyses extend posterior to the centra, and prezygapophyses are restricted and do not extend beyond the corresponding centra. As in other paravians such as *Microraptor*, *Archaeopteryx*, *Sinovenator,* and *Mei* (Xu et al., 2002; Xu and Norell, 2004; Hwang et al., 2002; Pei et al., 2014), the neural spines are prominent and located at the posterior portion of the neural arches. The centra of the posterior dorsal vertebrae are elongate and bear lateral concavities as in *Archaeopteryx* and dromaeosaurids (Wellnhofer, 2009; Turner et al., 2012). A lateral ridge is developed on the centrum at the base of the neural arch, and the transverse process is weakly developed.

FIGURE 11. Cervical series of BMNHC PH804.

FIGURE 12. Cervical series of BMNHC PH822.

FIGURE 13. Trunk region of PKUP V1068.

FIGURE 14. Trunk region of BMNHC PH804.

Twelve dorsal vertebrae are preserved in BMNHC PH804 (fig. 14). All of the dorsal vertebrae are exposed laterally. The centra of the anterior and middle dorsal vertebrae are short and those of the posterior vertebrae are elongate. In the middle dorsal vertebrae, the neural spines are high and anteroposteriorly long. The neural arch is twice the height of the corresponding centrum, which is in common in other paravians such as *Archaeopteryx*, *Sinovenator*, and *Microraptor* (Hwang et al., 2002; Xu et al., 2002; Wellnhofer, 2009). The prezygapophyses and postzygapophyses are lifted above the neural arches, and are anterodorsally and posterodorsally directed, respectively, in lateral view. Epipophyses are observed dorsal to the postzygapophyses, proximal to the articular facet. The lateral sides of the centra are concave but not pneumatic, as in PKUP V1068 and *Archaeopteryx*. The neural spines of the middle and posterior dorsal vertebrae have slightly anteroposteriorly expanded dorsal edges in lateral view (fig. 14), as in *Archaeopteryx* (Wellnhofer, 1974, 2009), but they are not as distinctly fan shaped as in compsognathids.

An estimated 12 dorsal vertebrae are present in BMNHC PH822 (fig. 15). The centra of the posterior dorsal vertebrae bear lateral concavities. The neural arch is twice as high as the centrum, as observed in BMNHC PH804. The neural spine is square, and positioned relatively posterior on the neural arch. The neural spine is relatively long, and approaches the neural spine of the preceding vertebra. The postzygapophyses are triangular in lateral view, and they extend posteriorly beyond the corresponding centra. Twelve dorsal vertebrae are also counted in BMNHC PH823 (fig. 16). The posterior dorsal vertebrae of both specimens have elongate centra, as in other specimens of this taxon.

FIGURE 15. Trunk region and humerus of BMNHC PH822.

A partial rib cage is preserved in BMNHC PH804 and BMNHC PH822 (figs. 14, 15), though some of the dorsal ribs and gastralia are displaced from their life position. No trace of uncinate processes is observed in these specimens. The dorsal ribs are grooved as in *Archaeopteryx* and *Microraptor* (Wellnhofer, 2009; Foth et al., 2014; Pei et al., 2014). As in *Archaeopteryx* and *Microraptor*, the anterior and posterior dorsal ribs of *Anchiornis* are shorter than the middle ones (Hwang et al., 2002; Xu et al., 2003; Wellnhofer, 2009; Pei et al., 2014). The longest dorsal ribs are associated with the 4th or 5th dorsal vertebra in BMNHC PH822, as in *Microraptor*, but in *Archaeopteryx* the longest dorsal ribs are associated with the 8th dorsal vertebra (Wellnhofer, 2009; Pei et al., 2014). The distal ends of the mid-dorsal ribs are slightly expanded as in *Archaeopteryx* and *Microraptor* (Wellnhofer, 2009; Foth et al., 2014; Pei et al., 2014), which possibly indicates joints for cartilaginous sternal ribs. Gastralia segments are also present in BMNHC PH804 and BMNHC PH822 (figs. 14, 15), but only a single set of elements is recognized, in contrast

FIGURE 16. Trunk region and humerus of BMNHC PH823.

to some dromaeosaurids, in which the gastralia has two sets of elements (Norell and Makovicky, 1997; Pei et al., 2014).

Sacral vertebrae: The sacral vertebrae of PKUP V1068 are preserved in ventral view (fig. 17). Five sacral vertebrae are present, which is typical of basal paravians (Xu, 2002; Wellnhofer, 2009). The middle three sacral vertebrae are fused together, while the 1st and 5th vertebrae are separated from the others. The centra of the sacral vertebrae are transversely broad. The ventral surface of the last three sacral vertebrae is flat. The middle three sacral vertebrae are apparently larger than the first and the last, as in the basal troodontid *Sinovenator* (Xu et al., 2002). Sacral ribs articulate with the brevis shelf in PKUP V1068. The 3rd sacral rib is slender, while the 2nd, 4th, and 5th sacral ribs are expanded. The exposed sacral vertebrae are all fused in BMNHC PH804, BMNHC PH822, and BMNHC PH823 (figs. 18–20). As observed in BMNHC PH823, the neural arches of the sacrum are fused, as in *Mei* (Xu and Norell, 2004; Gao et al., 2012).

Caudal vertebrae: The caudal vertebrae are laterally preserved in PKUP V1068 (fig. 21A). Twenty-two caudal vertebrae are exposed in PKUP V1068, less than in other *Anchiornis* specimens, in which over 30 caudal vertebrae are usually preserved. The anteriormost caudal vertebrae are not exposed in PKUP V1068, due to preservation. The articulations of the caudal and the sacral vertebrae are obfuscated by the pubis, and thus it is difficult to determine which caudal vertebra is the first. The anteriormost exposed caudal vertebrae are of comparable length to the posterior dorsal vertebrae (figs. 17, 21), which indicates that more proximal caudal vertebrae are not exposed in PKUP V1068. In other *Anchiornis* specimens (Xu et al., 2009; Hu et al., 2009), the proximalmost caudal vertebrae are significantly shorter than the posterior dorsal vertebrae. This is also the condition of *Archaeopteryx* and troodontids (e.g., Xu and Norell, 2004; Wellnhofer, 2009). The 6th exposed caudal vertebra reaches the maximum centrum length, while in other specimens the longest centrum is among the 12th–14th caudal

FIGURE 17. Pelvic region of PKUP V1068.

vertebrae. The transition point from shorter anterior vertebrae to longer middle and posterior vertebrae is difficult to determine in this specimen, because all exposed caudal vertebrae are relatively elongate. The transition point, if it is exposed, should be around the first or second exposed caudal vertebra. The longest caudal vertebra is about 1.5 times the length of the last posterior dorsal vertebrae in PKUP V1068. The centra of the middle and distal caudal vertebrae are elongate. As in *Archaeopteryx*, the caudal prezygapophyses of PKUP V1068 are reduced,

FIGURE 18. Pelvic girdle and femora of BMNHC PH804.

and reach only about one-fourth the length of the preceding vertebrae and, therefore, are not as extended as those in troodontid and dromaeosaurid dinosaurs. The centra of the caudal vertebrae are shallow. After the 6th exposed caudal vertebrae, the centra begin to reduce in length and thickness (fig. 21A).

In BMNHC PH804, 31 to 32 caudal vertebrae are preserved (fig. 22), as in the holotype (Xu et al., 2009). This is a higher number than in *Archaeopteryx*, dromaeosaurids, and troodontids (Norell and Makovicky, 2004; Makovicky and Norell, 2004). The anterior caudal vertebrae are short and square, with broad transverse processes as in *Microraptor*, but different from the elongate transverse processes of troodontids (Currie and Dong; 2001; Hwang et al., 2002; Pei et al., 2014; Norell et al., 2009). The anteriormost caudal vertebrae are significantly shortened, as in basal paravians, with only about two-thirds the length of the posterior dorsal vertebrae. The centra of the middle and posterior caudal vertebrae are elongate. The transition from anterior to middle and posterior caudal vertebrae begins on the 6th–8th caudal vertebrae, which is slightly distal compared to

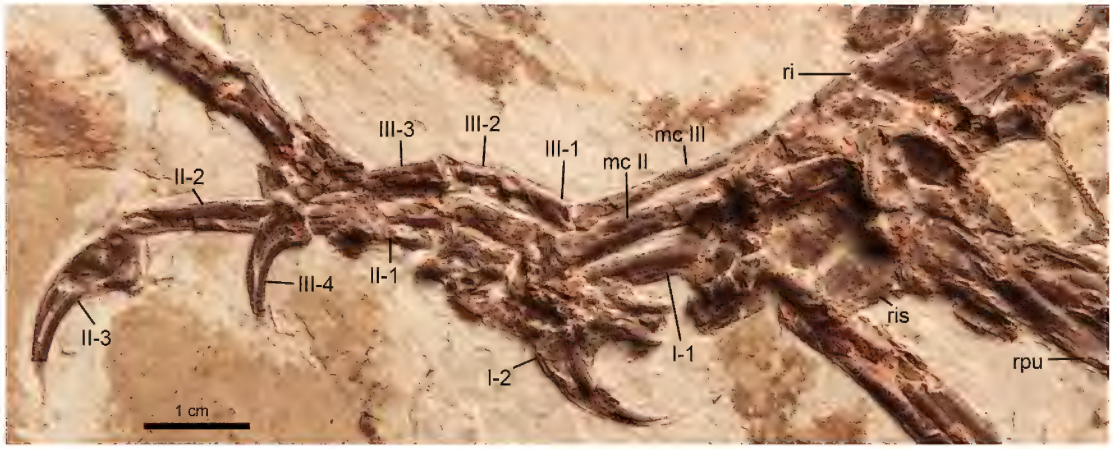

FIGURE 19. Pelvic region and left manus of BMNHC PH822.

Archaeopteryx (5th–6th caudal vertebrae), but more proximal than in troodontids (9th–10th caudal vertebrae) except for *Jinfengopteryx* (Ji and Ji, 2007). The centrum reaches a maximum length at the 13th–14th caudal vertebrae. The prezygapophyses can reach one-fourth the length of the previous centrum, which is much shorter than in dromaeosaurids (Norell and Makovicky, 2004). The posterior caudal vertebrae are concave laterally. The neural spine of the 12th caudal vertebra is visible as a low ridge in lateral view (fig. 22). This is similar to *Archaeopteryx* and dromaeosaurids, where the neural spine of each posterior caudal vertebra is reduced to a low ridge (Norell and Makovicky, 1999; Wellnhofer, 2009; Turner et al., 2011), but in contrast to troodontids, in which the neural spine becomes a sulcus along the neural arch of posterior caudal vertebrae (Xu et al., 2002; Norell et al., 2009). The chevrons associated with the anterior caudal vertebrae are reduced and platelike, similar to *Archaeopteryx*, but different from the rodlike anterior chevrons of deinonychosaurians (Norell and Makovicky, 1997; Wellnhofer, 2009; Norell et al., 2009). The chevrons become anteroposteriorly elongate beginning at the 7th caudal vertebra.

Thirty to 31 caudal vertebrae are estimated to be present in BMNHC PH822 (fig. 21B). The morphology of the caudal column is identical to BMNHC PH804. The anteriormost caudal vertebrae are reduced and bear broad transverse processes. The elongation of caudal vertebra begins at the 6th–8th caudal vertebrae like BMNHC PH804. The anterior chevrons are short and platelike. Distal chevrons are bifurcated anteriorly and single headed posteriorly. The prezygapophyses are elongate on posterior caudal vertebrae, and can reach one-fourth the length of the previous centra. At least 31 caudal vertebrae are preserved in BMNHC PH823, since the proximalmost caudal vertebrae are reconstructions (fig. 21C). The transition between the shorter anterior caudal vertebrae and longer posterior caudal vertebrae likely begins at the 6th–8th vertebrae, as in BMNHC PH804 and in BMNHC PH822. The centra are laterally concave except for the distalmost caudals.

Pectoral girdle: The furcula is boomerang shaped in PKUP V1068 (fig. 13), as in *Microraptor*, *Archaeopteryx,* and *Xiaotingia* (Hwang et al., 2002; Xu et al., 2011; Rauhut, 2014). As in *Microraptor* and *Archaeopteryx*, the ventral margin of the furcula is rounded, in contrast to *Mei* and *Oviraptor* in which a prominent hypocleidium is developed (Hwang et al., 2002; Xu and Norell, 2004; Nesbitt et al., 2009; Rauhut, 2014). A U-shaped furcula is also exposed in BMNHC PH804, with a smooth and rounded ventral margin. The fur-

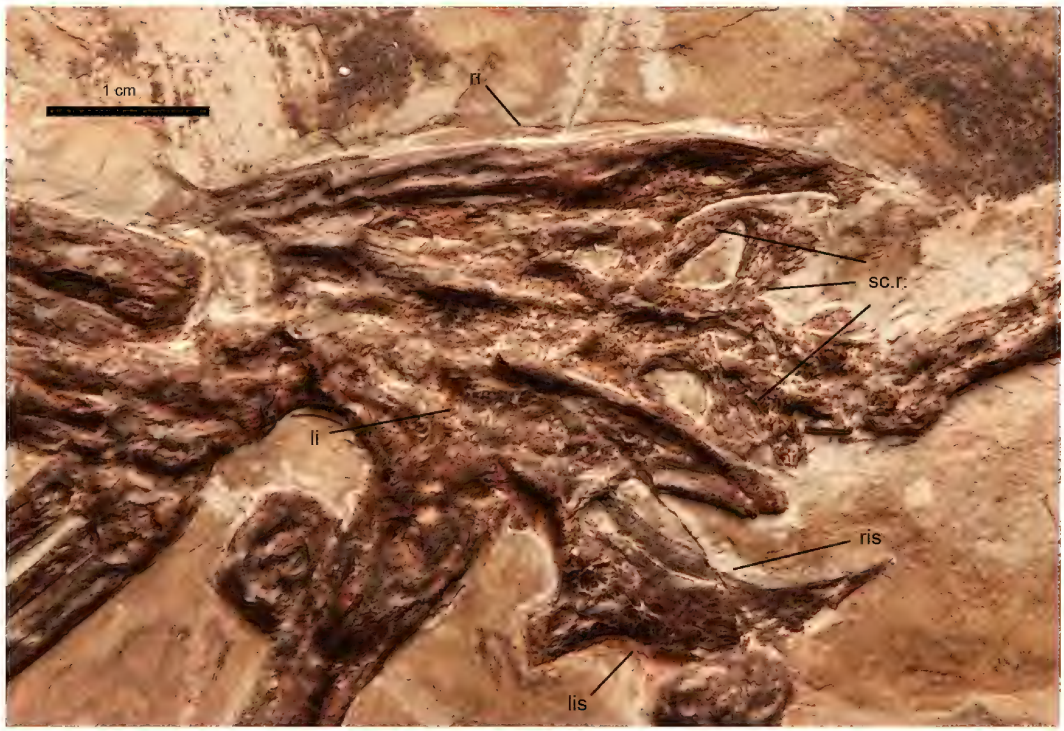

FIGURE 20. Pelvic region of BMNHC PH823.

cula is anteroposteriorly flattened in BMNHC PH822, and has rounded ends (fig. 14). The furcula bears an anterior groove in BMNHC PH822, but whether this is a preservational artifact is unknown.

In contrast to dromaeosaurids and derived avialans, no trace of an ossified sternum is observed in these specimens of *Anchiornis*, as in *Archaeopteryx* and troodontids, where an ossified sternum is also not preserved (Zheng et al., 2014).

Both scapulae are preserved in PKUP V1068. Their distal ends are eroded (fig. 13). The scapula is slender, at less than half of the humeral thickness. Unlike in deinonychosaurians, such as *Mei*, *Microraptor,* and *Linheraptor* (Xu and Norell, 2004; Xu et al., 2010; Pei et al., 2014), the scapula is significantly shortened in *Anchiornis huxleyi*, being around half the length of the humerus, which is also the condition of *Archaeopteryx* and *Xiaotingia* (Wellnhofer, 2009; Xu et al., 2011). The right scapula has a curved scapular blade in dorsal view, as in *Archaeopteryx*, *Mahakala,* and *Rahonavis* (Forster et al., 1998; Wellnhofer, 2009; Turner et al., 2011), while the left scapular blade is straight in lateral view in PKUP V1068 (fig. 13). The acromion process of PKUP V1068 is small as in other paravians such as *Archaeopteryx*, *Xiaotingia,* and *Sinornithoides* (Currie and Dong, 2001; Wellnhofer, 2009; Xu et al., 2011). The acromion is laterally everted as in basal paravians including *Xiaotingia*, and it projects smoothly from the scapular blade, extending anteriorly beyond the scapula-coracoid suture as in *Rahonavis* and *Sinovenator* (Forster et al., 1998; Xu et al., 2002). Posterior to the acromion, the scapula blade is distinctively depressed on the medial edge, a condition also present in *Xiaotingia* and *Sinovenator* (Xu et al., 2002, 2011). In BMNHC PH804, the left scapula is completely preserved and exposed in lateral view (fig. 14). It is slightly bowed and about half the length of the humerus as in the holotype (Xu et

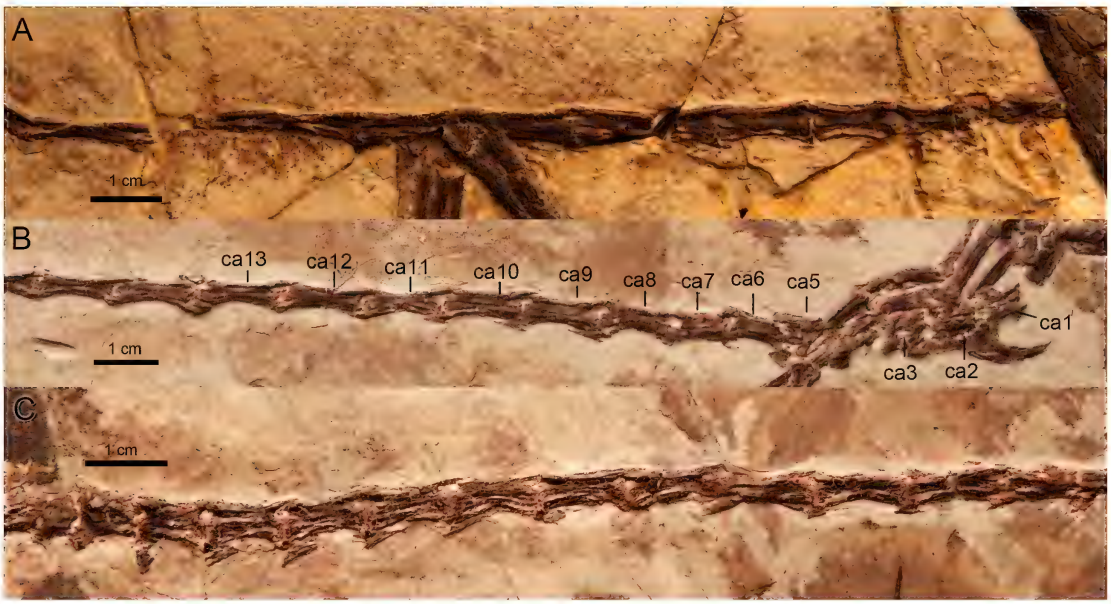

FIGURE 21. **A,** proximally exposed caudal vertebrae of PKUP V1068; **B,** proximal caudal vertebrae of BMNHC PH822; **C,** proximal caudal vertebrae of BMNHC PH823.

al., 2009). The scapular blade is bandlike and has a rounded distal end. The laterally everted acromion overhangs a groove along the lateral surface of the scapula as in *Sinovenator* and *Sinornithoides* (Currie and Dong, 2001; Xu et al., 2002). The scapula of BMNHC PH822 is curved in lateral view as in BMNHC PH804 (fig. 14). A shallow concavity is present between the acromion and the glenoid fossa as observed in other *Anchiornis* specimens. In BMNHC PH823, the ventral margin of the scapula is grooved near the glenoid fossa, as in *Xiaotingia* and other deinonychosaurians (fig. 16). The ventral rim of the scapular blade is thick.

Only the dorsal edge of the right coracoid is exposed in PKUP V1068 (fig. 13). The right coracoid of BMNHC PH804 is exposed in posterior/dorsal view (fig. 14). The scapula and the coracoid remain unfused. The coracoid is semisquare, and bares a distinct ventral curve like that of the holotype, as is typical of paravians (Currie and Dong, 2001; Xu and Norell, 2004; Xu et al., 2009). The posterior surface of the coracoid is rugose. In BMNHC PH822, the right coracoid is partially exposed in anterior/ventral view. It is associated with the scapula but remains unfused (fig. 15). The exact shape of the coracoid is ambiguous due to the poor preservation. The anterior/ventral surface of the coracoid is rugose, probably representing the condition of "numerous small pits sculptured on the ventral surface of the coracoid" as in the holotype IVPP V14378 (Xu et al., 2009).

Humerus: Both humeri are well preserved in PKUP V1068, and are exposed in posterolateral view (figs. 23, 24). The proximal end of the humerus is slightly expanded. The deltopectoral crest is proximally positioned, making up about one-sixth the length of the humeral shaft (fig. 24), as in the holotype (Xu et al., 2009). The deltopectoral crest is proportionally short compared with most other paravians, but is a common feature in other Late Jurassic paravians from the Jianchang area, such as *Xiaotingia*, *Aurornis,* and *Eosinopteryx* (Xu et al., 2011; Godefroit, et al., 2013a, 2013b). An extremely reduced deltopectoral crest is also present in ornithomimids (Makovicky et al., 2004). The

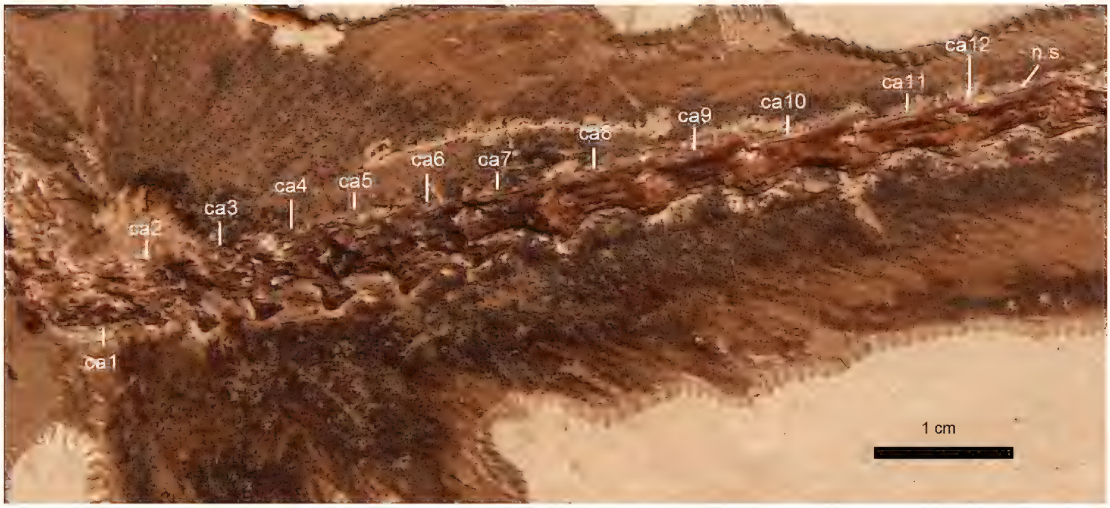

FIGURE 22. Proximal caudal vertebrae of BMNHC PH804.

humeral shaft of PKUP V1068 is straight, and about 1.2 times the length of the ulna. The diameter of the humeral shaft remains constant except at the distal end, where it curves anteriorly and becomes anteroposteriorly flattened in lateral view (figs. 22, 23). This feature is observed in all *Anchiornis* specimens, and a distinct curvature at the distal end of humerus is also present in many basal paravians such as *Rahonavis*, *Mei,* and *Archaeopteryx* (O'Connor and Forster, 2000; Xu and Norell, 2004; Foth et al., 2014). The radial condyle is weakly developed in lateral view, and a weak ectepicondyle attaches to the radial condyle anteriorly. The entire forelimb, including the humerus, is elongate in *Anchiornis* compared to dromaeosaurids and troodontids, which is a primitive condition for basal paravians (Currie and Dong, 2001; Xu and Norell, 2004; Zhang et al., 2008; Turner et al., 2012). As in the *Anchiornis huxleyi* holotype, but, unlike in *Archaeopteryx* and derived avialans (Chiappe et al., 1999; Xu et al., 2009; Wellnhofer, 2009; Zhou and Zhang, 2003), the humerus is shorter than the femur in PKUP V1068.

The left humerus is straight in posterolateral view in BMNHC PH804 (fig. 25). The deltopectoral crest is short, as in PKUP V1068. Distally, the posterior edge of the humerus curves anteriorly, but the radial condyle is relatively larger than in PKUP V1068. A groove is present along the right humeral shaft posteriorly in BMNHC PH804 (fig. 26). Both BMNHC PH822 and BMNHC PH823 have a reduced deltopectoral crest, as in the holotype and other specimens of *Anchiornis* (figs. 15, 16). In BMNHC PH822, the humerus is straight along most of the shaft, but the distal end of the humerus curves anteriorly in lateral view as in other specimens of *Anchiornis* (fig. 15). The humeral shaft of BMNHC PH823 is slightly sinusoidal and not as straight as in other specimens (fig. 16).

Ulna and radius: Both the right and left ulnae and radii are well exposed in PKUP V1068 (figs. 23, 24). The ulna and radius are straight, as in the *Anchiornis* type specimen and *Archaeopteryx* (Wellnhofer, 1974; Xu et al., 2009). The ulna is slender and shorter than the humerus, and slightly more robust than the radius, as in *Archaeopteryx* and troodontids, but differs from many dromaeosaurids in which the radius is considerably thinner than the ulna (Xu, 2002; Hwang et al., 2002; Turner et al., 2012). The diameter of the midshaft of the left ulna is about 60% of the humerus and 120% of the radius. The proximal end of the ulna is slightly expanded, with a weak olecranon pro-

FIGURE 23. Left forelimb of PKUP V1068.

cess. The ulna shaft is mostly straight, with the distal end slightly bowed inward. This is different from some other paravians (e.g., *Mei* and *Microraptor*), where the ulna is distinctly bowed both proximally and distally (Gauthier, 1986; Xu and Norell, 2004; Pei et al., 2014). The radius is shorter and more slender than the ulna in PKUP V1068. The radius is straight, with both ends slightly expanded. The distal end of the radius has a flat contact face with the radiale. In BMNHC PH804, BMNHC PH822, and BMNHC PH823, both the ulna and the radius are straight, and the ulna is only slightly more robust than the radius (figs. 25–27). The morphology of the ulna and the radius are identical as in PKUP V1068 (figs. 25–27).

Carpals: In PKUP V1068, the radiale is a thick disklike element, positioned between the radius and the semilunate (figs. 28, 29). It has a flat proximal surface and rugose distal surface on the left wrist. In the right wrist, a stout carpal between the semilunate and the medial condyle of the radius may represent the radiale.

The semilunate of PKUP V1068 is larger than the radiale. It is subtriangular to crescent shaped in dorsal view (fig. 29). Proximally, it contacts the radiale. Distally the semilunate covers the proximal end of metacarpals I and II on the left manus, and possibly slightly contacts metacarpal III, as in the referred specimen LPM-B00169 and some paravians, such as *Deinonychus* (Ostrom, 1969; Gishlick, 2001; Hu et al., 2009). This condition differs from the holotype where the semilunate appears attached only on metacarpal II and metacarpal III. On the right wrist, the semilunate covers the proxi-

FIGURE 24. Right forelimb of PKUP V1068.

mal end of metacarpal II, and possibly contacts both metacarpals I and III. As a contrast, the semilunate contacts only metacarpals I and II in *Archaeopteryx* (Wellnhofer, 2009).

In BMNHC PH804 the radiale is a platelike element located between the semilunate and the radius (fig. 25). In the left wrist of BMNHC PH804, the semilunate contacts the proximal end of metacarpal I and II (fig. 25), as in PKUP V1068. In BMNHC PH822, a disklike radiale is present on the right wrist (fig. 30). The semilunate is centered on the proximal end of metacarpal II, but possibly contacts metacarpal I and metacarpal III as well. Considering the various positions of the semilunate observed in different *Anchiornis* specimens, this variation is likely a preservational artifact (also see in the Discussion).

Manus: The manus of *Anchiornis* is elongate as in *Xiaotingia* and *Archaeopteryx* (Wellnhofer, 1974; Xu et al., 2011). In PKUP V1068, metacarpal I is the shortest metacarpal, and closely attaches to metacarpal II (figs. 28, 29). The dorsal surface of metacarpal I is flat on the right manus, but bears a groove on the left manus (possibly due to postmortem compression). A sharp ridge is developed dorsomedially on the proximal half of the metacarpal I shaft as in *Archaeopteryx* and *Sinornithoides* (Wellnhofer, 1974; Currie and Dong, 2001). The shaft of metacarpal II is straight, with both ends expanded. The distal end of meta-

FIGURE 25. Left forelimb of BMNHC PH804.

carpal II bears two condyles, and the medial condyle is more developed than the lateral condyle. The diameter of the shaft is about the same as metacarpal I. Metacarpal III is slender and slightly shorter than metacarpal II, as in other paravians. It is distinctly bowed in PKUP V1068, as in *Xiaotingia* (Xu et al., 2011). A slight curvature of metacarpal III is also observed in the *Anchiornis* holotype and the referred specimen LPM-B00169 (Xu et al., 2009; Hu et al., 2009), as well as in *Archaeopteryx* and some other maniraptorans such as *Sinornithoides*, *Velociraptor,* and *Deinonychus* (Ostrom, 1969; Wellnhofer, 1974; Norell and Makovicky, 1999; Currie and Dong, 2001;

FIGURE 26. Right forelimb of BMNHC PH804.

Gishlick, 2001). Unlike in *Xiaotingia*, but as in other paravians, metacarpal III is more slender than metacarpal II (Xu et al., 2011). The proximal end of metacarpal III is slightly expanded.

Phalanx I-1 is slightly bowed in PKUP V1068. It is about 70% the length of metacarpal II, but with the same thickness as metacarpal II (figs. 28, 29). A deep and round ligament pit is present on the distal condyle of phalanx I-1. As in *Archaeopteryx* but differing from the condition in *Microraptor*, phalanx II-1 is shorter than phalanx II-2 (Hwang, et al., 2002; Foth et al., 2014). Phalanx II-2 is about the same length as phalanx I-1, and is slightly curved, as in the holotype and LPM-B00169 (Xu et al., 2009; Hu et al., 2009). The shaft of phalanx II-1 has a roughly constant diameter, but the shaft of phalanx II-2 decreases distally. Phalanx III-1 and phalanx III-2 are the shortest phalanges, and are slightly bowed on the left manus. Phalanx III-3 is also ventrally curved, and it is longer than phalanx III-1 and phalanx III-2 combined, as is typical of paravians (Wellnhofer, 1974; Norell and Makovicky, 1999).

Manual ungual phalanges of PKUP V1068 are distinctly curved as in most paravians. Unlike advanced maniraptorans (including *Archaeopteryx*), the manual claws are not markedly upcurving, which represents a primitive condition of coelurosaurians. Ungual phalanx I-2 has a curvature over 90°, and it articulates phalanx I-1 on the dorsal half of its proximal end. The articular facet is more dorsally placed on ungual phalanx II-3 compared with ungual phalanx I-2. Ungual phalanges I-2 and II-3 are about the same size, while phalanx III-4 is the smallest and is not as curved as phalanx I-2 (fig. 29). A proximodorsal lip is present immediately dorsal to the articular surface of each ungual phalange, as in other pennaraptorans (Foth et al., 2014).

In BMNHC PH804, the right metacarpals are not well exposed, and the left metacarpals are not fully prepared (figs. 25, 26). Phalanges I-2 and II-2 appear to be curved in the left manus, as in other specimens of *Anchiornis*. The ungual phalanx is relatively small and not as curved compared with other *Anchiornis* specimens. The articular surface of ungual phalanx II-3 is dorsally located. As in PKUP V1068, each ungual phalange has distinct proximodorsal lip.

In BMNHC PH822, metacarpal I is one-third the length of metacarpal II, and is relatively shorter than in PKUP V1068. Metacarpal III is

slender and straight in dorsal view (figs. 30, 31). Phalanx I-2 appears more robust than metacarpal II. Phalanges I-2, II-3, and III-4 are straight on the right manus, but slightly curved on the left manus, probably due to the angle of observation. For ungual phalanx II-3, the articular facet is dorsally positioned and it makes up less than one-third the posterior edge of the phalanx. The ungual phalanges are distinctly curved and bear distinct proximodorsal lips, as in the holotype and PKUP V1068.

Ilium: The pelvic girdle is preserved in ventral view in PKUP V1068, unlike the rest of the skeleton, which is mostly exposed in dorsal view. The right ilium is deformed due to compression, and preserved as a bone sheet (fig. 17). The right ilium is about half the length of the femur.

In BMNHC PH804, the left ilium is well exposed in lateral view (fig. 18). The anterior process has a squared anterior end, as in the holotype and dromaeosaurids, but differing from *Xiaotingia* and *Archaeopteryx* in which the anterior end of the ilium is more rounded (Norell and Makovicky et al., 1999; Xu et al., 2009, 2011). The anterior tip of the anterior process is slightly ventrally hooked, as in the holotype (Xu et al., 2009). The posterior process projects horizontally, except for a slight ventral curvature at the posterior end as in many dromaeosaurids (Norell and Makovicky, 1999; Burnham et al., 2000; Turner et al., 2011; Pei et al., 2014). As a contrast, this ventral curvature is absent in the basal troodontids such as *Sinovenator*, *Mei,* and *Jinfengopteryx* (Xu et al., 2002; Xu and Norell, 2004; Ji et al., 2005; Gao et al., 2012). As in *Archaeopteryx* (Wellnhofer, 1974, 2009), the cuppedicus fossa of BMNHC PH804 is broadly exposed anterior to the pubic peduncle and faces laterally. It is proportionally larger than in basal deinonychosaurians like *Sinovenator* and *Mahakala* (Xu et al., 2002; Turner et al., 2007, 2011). The pubic peduncle is larger than the ischiadic peduncle, and is more ventrally extended, as in *Archaeopteryx* and troodontids (Wellnhofer, 1974; Xu et al., 2002; Tsuihiji et al., 2014). The acetabulum bears a mediodorsal wall, which is also observed

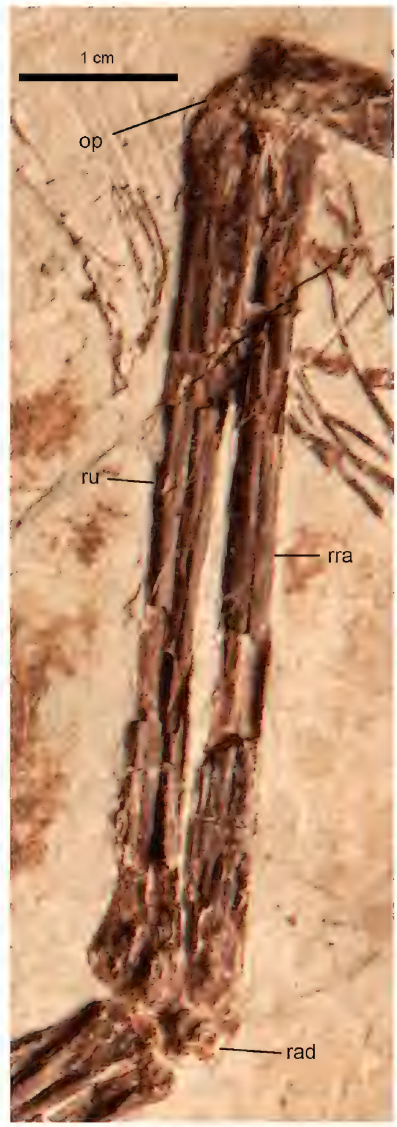

FIGURE 27. Right ulna and radius of BMNHC PH822.

in the holotype IVPP V14378 and BMNHC PH822 (Xu et al., 2009).

The right ilium is exposed in lateral view in BMNHC PH822 (fig. 19). The anterior process extends horizontally and slightly curves ventrally at the anterior end. The anterodorsal margin of the anterior process is damaged, and the ilium probably has a square anterior end as in the other *Anchiornis* specimens. The posterior

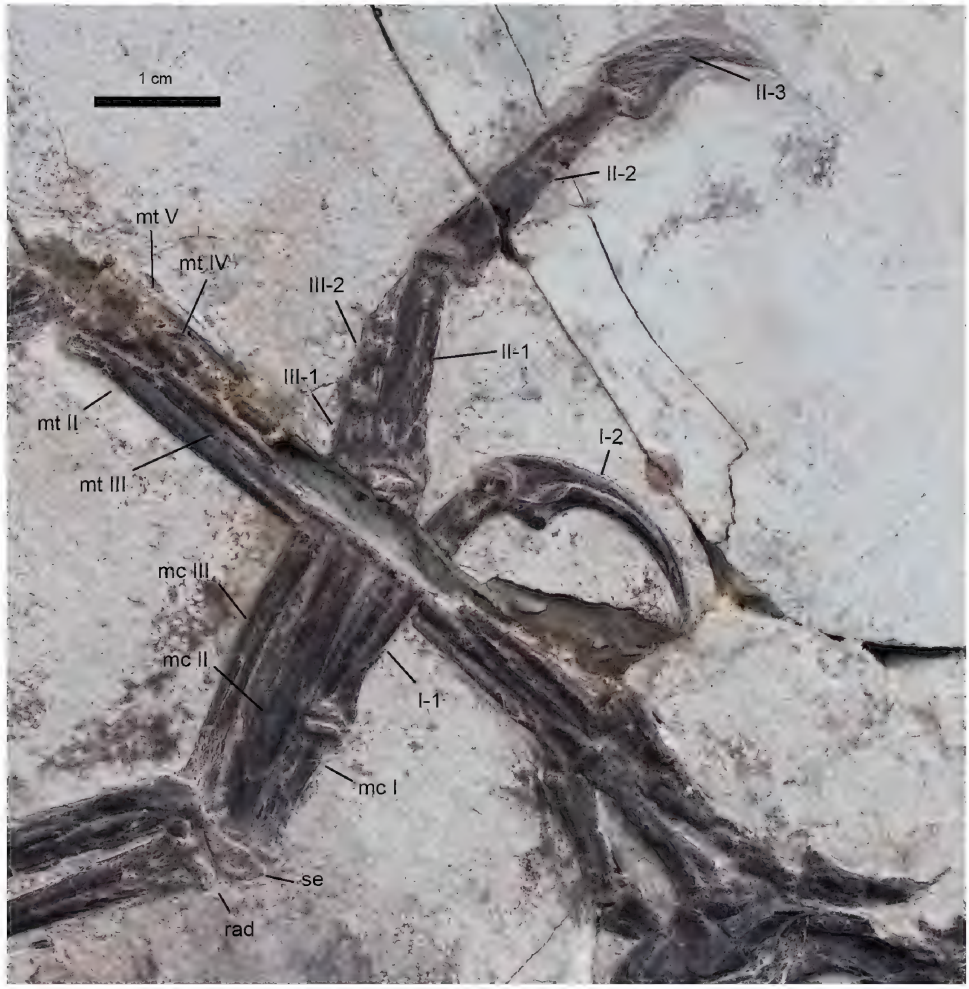

FIGURE 28. Left manus of PKUP V1068.

and anterior processes are subequal in size. The posterior end of the ilium forms an acute angle. A supraacetabular crest is developed, as in the holotype and LPM-B00169 (Xu et al., 2009; Hu et al., 2009). The pubic peduncle is anteroposteriorly expanded and extends more ventrally than the ischiadic peduncle, as in BMNHC PH804 and LPM-B00169 (Hu et al., 2009). A laterally faced cuppedicus fossa is developed anterior to the pubic peduncle. A horizontally oriented brevis shelf is developed ventral to the postacetabular blade.

In BMNHC PH823, both ilia are well preserved (fig. 20). The paired ilia approach each other anteriorly in dorsal view. The angle between the ilia is about 30° in dorsal view. The anterodorsal edge of the ilium is damaged and its shape is hard to determine, but it curves slightly ventrally as in LPM-B00169. The posterior process is slightly longer than the anterior process, and also ventrally curves at the tip, as in LPM-B00169 and dromaeosaurids (Hwang et al., 2002; Hu et al., 2009; Turner et al., 2011). The ventral curvatures of the anterior and posterior tips of the ilia are also present in dromaeosaurids such as *Mahakala*, *Microraptor*, but only an anterior curvature is present in troodontids such as *Sinovenator* (Xu et al., 2000, 2002; Turner et al., 2007).

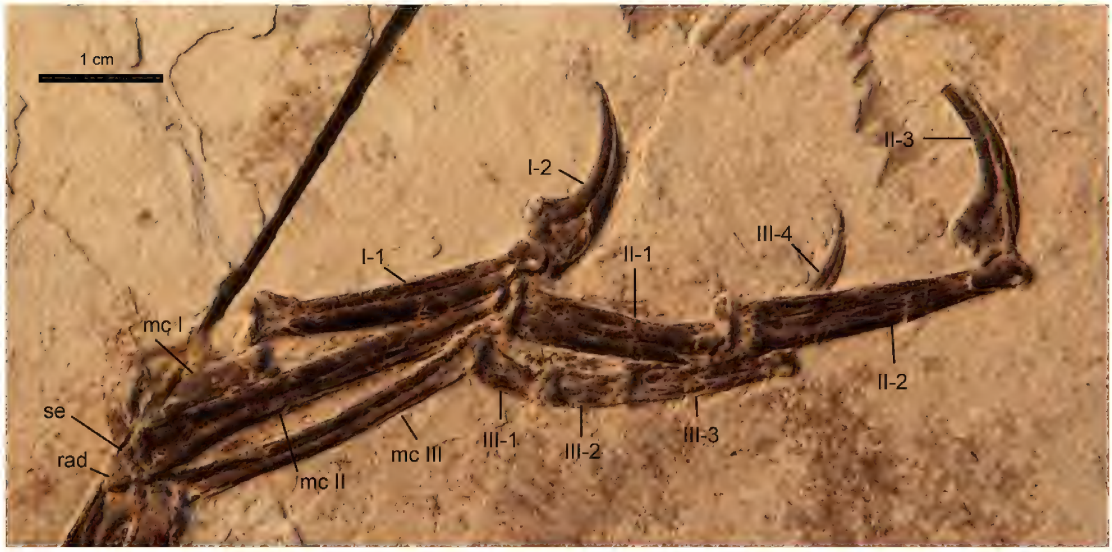

FIGURE 29. Right manus of PKUP V1068.

Pubis: The pubes of PKUP V1068 are articulated with each other distally, and exposed in anterior view (fig. 17). The orientation of the pubis is unknown due to compression. The pubis is about 80% the length of the femur. The pubic shaft is bowed as in other paravians, such as *Archaeopteryx*, *Sinovenator,* and *Microraptor* (Wellnhofer, 1974; Xu et al., 2002; Xu et al., 2003). It is mediolaterally flat near the proximal end, but becomes rounded at the midshaft, and is anteroposteriorly flat distally. The pubic apron is developed from the distal one-third of the pubis, as in *Archaeopteryx*, but is proportionally shorter than in *Sinovenator* (Xu et al., 2002; Wellnhofer, 2009). The pubic apron of PKUP V1068 lacks the slitlike opening present in deinonychosaurians, such as *Sinovenator* and *Velociraptor* (Norell and Makovicky, 1999; Xu et al., 2002). The pubic boot of PKUP V1068 has no anterior expansion. The lateral edge of the pubis is smooth, and does not bear a lateral ridge such as the one that is present in some basal troodontids and some basal dromaeosaurids like *Sinovenator* and *Microraptor* (Xu et al., 2002; Pei et al., 2014).

The pubis of BMNHC PH804 is ventrally oriented as in basal deinonychosaurians (fig. 18) (Norell and Makovicky, 2004). It is mediolaterally flat proximally, but twists to become anteroposteriorly flat at the midshaft. The pubic boot is rounded anteriorly and expanded posteriorly. The posterior expansion of BMNHC PH804 is bladelike, more prominent than in the referred specimen LPM-B00169, and similar to some dromaeosaurids, such as *Bambiraptor* (Burnham et al., 2000; Hu et al., 2009). A large and posteriorly expressed pubic boot is also present in *Unenlagia* and *Archaeopteryx* (Novas and Puerta, 1997; Foth et al., 2014).

The pubis is anteroventrally positioned in BMNHC PH822 (fig. 32). The pubis is bowed and about 80% the length of the femur in lateral view, as in PKUP V1068. Proximally, the pubic shaft is anteroposteriorly expanded and distally it is mediolaterally flat. The pubic boot is anteroventrally rounded, but with a prominent posterior expansion, as in BMNHC PH804.

Ischium: The ischia are not well exposed in PKUP V1068 or BMNHC PH822. Both ischia are present in BMNHC PH804 (fig. 18). The ischial shaft is short, about one-third the length of the pubis, which is typical in *Anchiornis*, and similar to that of *Aurornis* and *Eosinopteryx* (Godefroit et al., 2013a, 2013b). In *Xiaotingia*, *Archaeopteryx,* and basal deinonychosaurians

FIGURE 30. Right manus of BMNHC PH822.

(Xu et al., 2002, 2011; Hwang et al., 2002; Foth et al., 2014), the ischium is also relatively short (about 50% the length of the pubis), but is not as reduced as in *Anchiornis*. The obturator process is located near the distal end of the ischiadic shaft in BMNHC PH804 (fig. 18), like *Xiaotingia*, *Archaeopteryx*, and basal deinonychosaurians (Wellnhofer, 1988; Hwang et al., 2002; Xu et al., 2002, 2011). As in the type specimen IVPP V14378 (Xu et al., 2009), the obtu-

FIGURE 31. Femora of PKUP V1068 and BMNHC PH823. **A,** left femur of PKUP V1068; **B,** right femur of PKUP V1068; **C,** left femur of BMNHC PH823; **D,** right femur of BMNHC PH823.

rator process of BMNHC PH804 has a ventrally pointed extension that is also present in *Archaeopteryx* and other Jianchang paravians such as *Xiaotingia*, *Aurornis,* and *Eosinopteryx* (Wellnhofer, 1988; Xu et al., 2011; Godefroit et al., 2013a, 2013b). The tip of the ventral extension is damaged in BMNHC PH804, but it appears rounded in the type specimen IVPP V14378 (Xu et al., 2009). The ischial shaft tapers posteroventrally in BMNHC PH804 and other *Anchiornis* specimens, including the type specimen (Xu et al., 2009).

The ischia in BMNHC PH823 are exposed in lateral view (fig. 20). It is reduced in length, about 30% the length of the femur. Proximally, the iliac and pubic peduncles are subequal in size, and the squared pubic peduncle projects further anteriorly. The lateral surface of the ischium is flat. An obturator process is present near the distal end of the shaft as in other basal paravians (Xu et al., 2002, 2011; Hwang et al., 2002; Godefroit et al., 2013b; Foth et al., 2014), while the ventral extension of the obturator process is not well exposed in this specimen. The posterior margin of the ischium is relatively smooth, lacking a distinct posterodorsal process that is present in *Rahonavis* (Forster et al., 1998). The distal end of the ischium tapers posteroventrally as in the type specimen (Xu et al., 2009).

FIGURE 32. Femora and right pubis of BMNHC PH822.

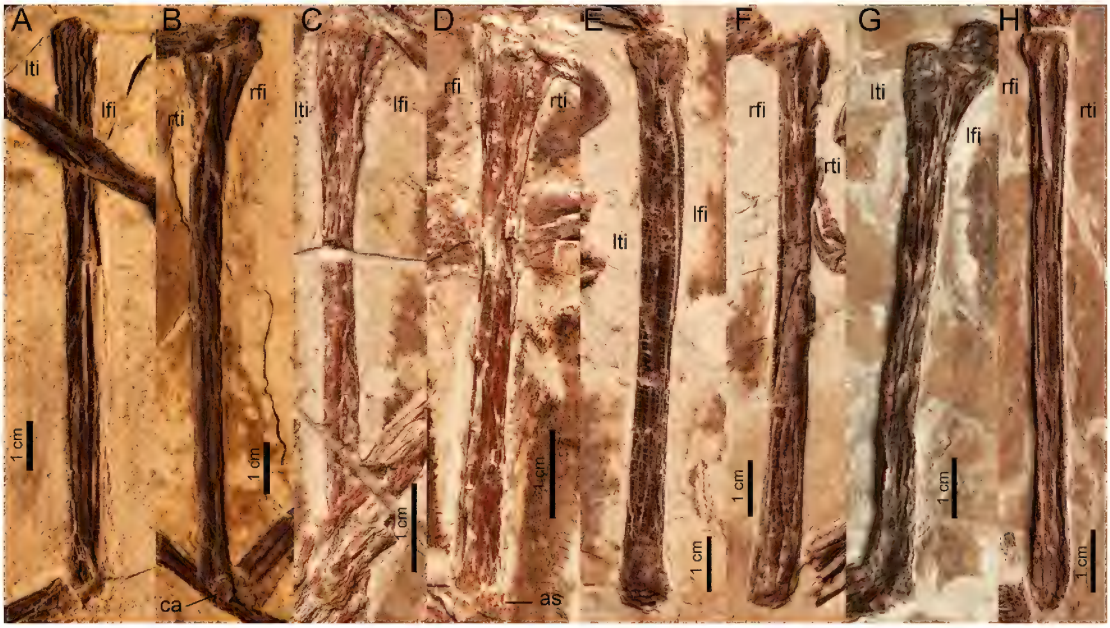

FIGURE 33. Tibiotarsi of BMNHC PH804, BMNHC PH822, BMNHC PH823, and PKUP V1068. **A,** left tibiotarsus of PKUP V1068; **B,** right tibiotarsus of PKUP V1068; **C,** left tibiotarsus of BMNHC PH804; **D,** right tibiotarsus of BMNHC PH804; **E,** left tibiotarsus of BMNHC PH822; **F,** right tibiotarsus of BMNHC PH822; **G,** left tibiotarsus of BMNHC PH823; **H,** right tibiotarsus of BMNHC PH823.

Femur: Both femora are well preserved in PKUP V1068 (fig. 31). The right femur is exposed in lateral view and the left femur is exposed in posterolateral view. The femur is anteriorly bowed, a typical condition of theropods (Gauthier, 1986). The femur of PKUP V1068 is elongate, about 150% length of the skull, which is relatively longer than other *Anchiornis* specimens and *Archaeopteryx*. However, this could be allometric variation. Distally, the lateral condyle of femur is rounded and projects anteriorly from the femoral shaft.

The femora are bowed in BMNHC PH804 (fig. 18), about 120% the length of the skull. The greater trochanter is separated from the lessor trochanter by a notch. The greater trochanter of BMNHC PH804 is more proximally positioned than the lesser trochanter as in other paravians such as *Archaeopteryx*, *Sinovenator,* and *Mahakala* (Wellnhofer, 1988; Xu et al., 2002; Turner et al., 2007). A sharp crest representing the posterior trochanter is developed distal to the base of the greater trochanter on the posterior side of the femur, as in other maniraptorans (e.g., Norell and Makovicky, 1997; Wellnhofer, 2009; Turner et al., 2011). In BMNHC PH822, the femur is about 125% the length of the skull. Unlike other *Anchiornis* specimens, the proximal end of the lesser trochanter appears higher than that of the greater trochanter (fig. 18), but this could be a preservational artifact (fig. 32). An ectocondyle is developed posterolateral on the distal end of the femur, separated from the lateral condyle by a shallow notch, which is a condition widely distributed in theropods. In BMNHC PH823. The lesser and greater trochanters are separated by a shallow groove (fig. 18). A posterior trochanter is developed distal to the great trochanter on the posterior side, as is typical of maniraptorans (fig. 31). The femur is about 125% the length of the skull in BMNHC PH823.

Tibiotarsus: Tibiae are well preserved in PKUP V1068, BMNHC PH804, BMNHC PH822, and BMNHC PH823 and have similar morphology in

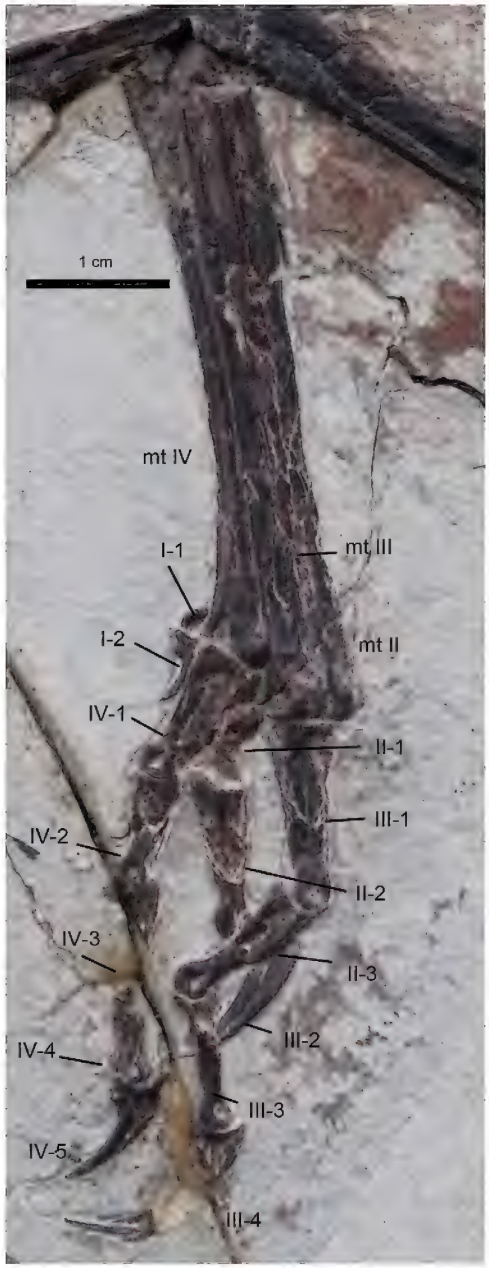

FIGURE 34. Right pes of PKUP V1068.

all specimens (fig. 33). The tibia is long and straight, about 140%–155% the length of the femur. Proximally the tibia is slightly expanded. The cnemial crest is moderately developed as in *Eosinopteryx* and *Sinovenator* (Xu et al., 2002; Godefroit et al., 2013a). Unlike *Archaeopteryx*, but similar to *Mahakala* and *Microraptor*, the distal end of the tibia is not significantly expanded (Hwang et al., 2002; Turner et al., 2007; Wellnhofer, 2009). The tibia is not fused with the proximal tarsals in PKUP V1068 and BMNHC PH804, and it is hard to determine whether they are fused in BMNHC PH822 and BMNHC PH823 due to poor preservation.

The fibula is present in all four specimens (fig. 33). Unlike many paravians, the proximal end of the fibula is significantly expanded and is anteroposteriorly broad at the proximal end of the tibia (fig. 33). A prominent anterior crest is developed on the proximal end of the fibula. An iliofibularis tubercle is present near to the proximal end of the fibula and projects laterally as observed in PKUP V1068. In BMNHV PH823, the medial surface of the proximal fibula is flat, and distally becomes slightly grooved.

An astragalus is exposed on the right side in BMNHC PH804 and is not fused to the tibia, like *Archaeopteryx* and many deinonychosaurians (e.g., Wellnhofer, 1993; Norell and Makovicky, 1997; Burnham et al., 2000; Zanno et al., 2011). The calcaneum is exposed on the left leg of PKUP V1068 (fig. 33). It is subtriangular in lateral view, and is not fused to the tibia. The calcaneum is square in lateral view in BMNHC PH823.

Pes: Both feet of PKUP V1068 are exposed in dorsolateral view (figs. 28, 34). The right metatarsals are slightly detached from each other and damaged on their proximal ends while the left metatarsals remain in life position except for breakage at midshaft (fig. 34). The metatarsus is nearly symmetric as in basal dromaeosaurids and *Archaeopteryx*, but unlike derived troodontids, in which the metatarsus is asymmetric with a significantly wider and longer metatarsal IV (Xu et al., 1999; Zanno et al., 2011). Metatarsal II is straight, slightly shorter than metatarsal III. Both ends of metatarsal II are slightly expanded,

and the distal end appears not ginglymoid. Proximally, metatarsal III is closely pressed by metatarsal II and metatarsal IV as observed in the left pes. However, the proximal end of metatarsal III is not pinched, and is as transversely wide as metatarsal II and metatarsal IV, and thus the subarctometatarsalian condition reported in the type specimen of *Anchiornis* (Xu et al., 2009) is not observed in PKUP V1068. A subarctometatarsalian pes is present in basal troodontids, *Sinornithosaurus,* and *Microraptor* (Xu et al., 1999, 2000, 2002; Makovicky and Norell, 2004), but is absent in avialans and other dromaeosaurids (Norell and Makovicky, 2004; Turner et al., 2012). The proximal end of metatarsal III is also exposed broadly in anterior view in the type specimen IVPP V14378 and the referred specimen LPM-B00169 (Xu et al., 2009; Hu et al., 2009), and it is not significantly constricted compared with metatarsal II and metatarsal IV, which resembles the condition of *Archaeopteryx* and *Mahakala* (Wellnhofer, 1974; Turner et al., 2011), but unlike the strongly pinched metatarsal III of *Sinovenator*, *Mei,* and *Microraptor* (Xu et al., 2000, 2002; Xu and Norell, 2004). Therefore, we considered the pes of *Anchiornis* as normal instead of arctometatarsalian in this study. The distal end of metatarsal III is ginglymoid in PKUP V1068, which is a primitive condition for paravians. Metatarsal IV is about the same size as metatarsal II. The proximal end of metatarsal IV is transversely expanded and appears broader than metatarsals II and III. Distally, metatarsal IV appears ginglymoid in shape (fig. 34). Metatarsal V is preserved proximally on the left foot (fig. 28). It is very slender and closely attaches to metatarsal IV posterolaterally. Metatarsal V is straight in *Anchiornis*, unlike the bowed metatarsal V in *Microraptor* and *Philovenator* (Hwang et al., 2002; Xu et al., 2012).

Only the partial distal end of phalanx I-1 is exposed on the right pes of PKUP V1068, which indicates metatarsal I is possibly attached to the posterolateral side of metatarsal II (fig. 34), as in *Microraptor*, *Aurornis,* and *Archaeopteryx* (Mayr et al., 2005, 2007; Godefroit et al., 2013b; Pei et

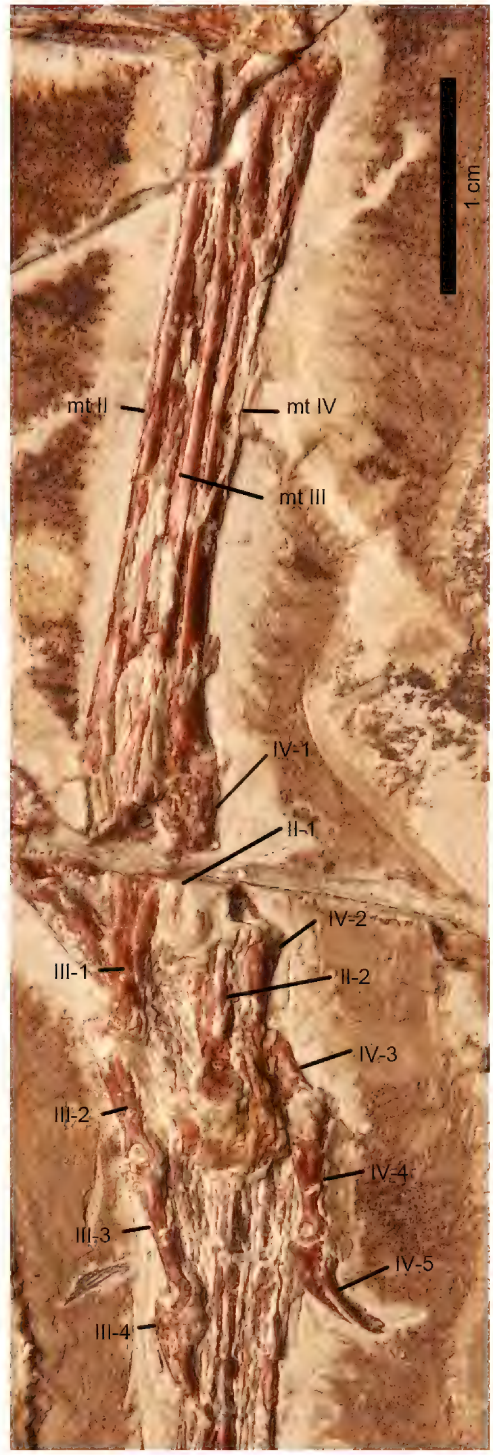

FIGURE 35. Left pes of BMNHC PH804.

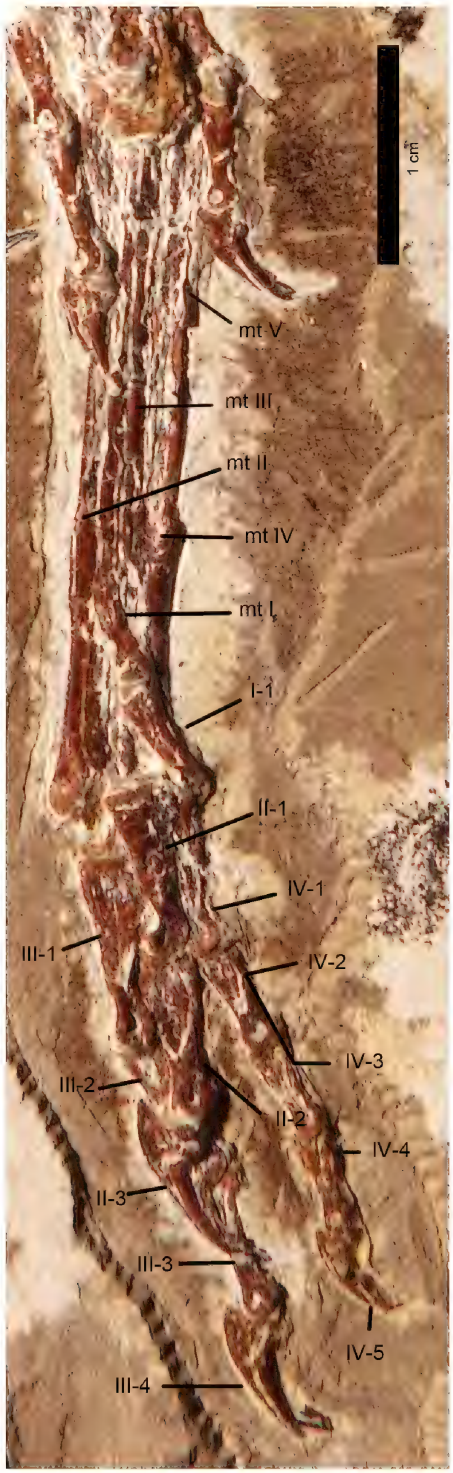

FIGURE 36. Right pes of BMNHC PH804.

al., 2014). Phalanx II-1 is similar in length of phalanx II-2, a primitive condition resembling that in *Archaeopteryx*, but differs from the condition in most deinonychosaurians, in which phalanx II-2 is significantly reduced (Gauthier, 1986; Makovicky and Norell, 2004; Norell and Makovicky, 2004; Turner et al., 2012; but see Csiki et al., 2010). Phalanx II-2 bears a weak ventral heel proximally, but the ventral heel is not as distinct as in derived deinonychosaurians (Makovicky and Norell, 2004; Norell and Makovicky, 2004). Phalanx III-1 is the longest and most robust phalanx, about 115% the length of phalanx II-1 (fig. 34). Phalanx III-2 is about the same size and shape as phalanx II-2, but with a more developed dorsal lip proximally. Phalanx III-3 is slender. The distal end is similar in size to phalanx III-2. Phalanx IV-1 is as robust as phalanx III-1, and is about the same length as phalanx II-2. A weakly developed constriction lies near the distal end of phalanx IV-1. Phalanx IV-2 is as slender as phalanx III-3, but is shorter, at about 70% the length of phalanx IV-1. Phalanx IV-3 and phalanx IV-4 are subequal in size and shape, and shorter than phalanx IV-2 (fig. 34).

Ungual phalanges I-2, II-3, III-4, and IV-5 have similar curvature (~70°) (fig. 34), smaller than and not as curved as manual ungual I-2 (>90°). Phalanx I-2 is the smallest ungual phalanx. A distinct proximodorsal lip is developed on ungual phalanges II-3, III-4, and IV-5. Phalanx II-3 is slightly more robust than III-4, as in the holotype, but not as distinctly enlarged as in derived troodontids and dromaeosaurids. Ungual phalanx IV-5 is smaller than II-3 and III-4.

In BMNHC PH804, metatarsal I appears short and slender (fig. 36). It is attached to metatarsal II posterolaterally, and is slightly distal to the midshaft of metatarsal II. Metatarsal I is not as distally located as it is in *Epidendrosaurus*, *Archaeopteryx,* and *Jeholornis*, but is similar to the condition in troodontids and dromaeosaurids such as *Mei*, *Talos,* and *Microraptor* (Zhang et al., 2002; Zhou and Zhang, 2002; Xu and Norell, 2004; Zanno et al., 2011; Foth et al., 2014; Pei et al., 2014). Metatarsals II and IV are subequal in length, while

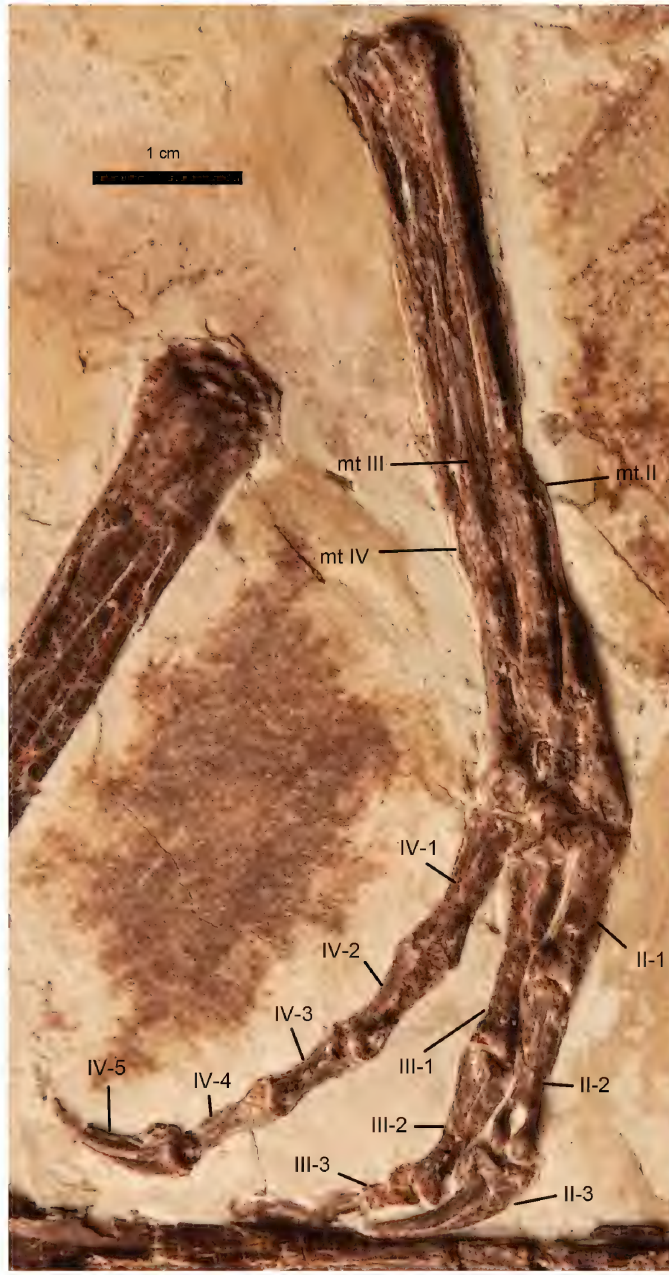

FIGURE 37. Left pes of BMNHC PH822.

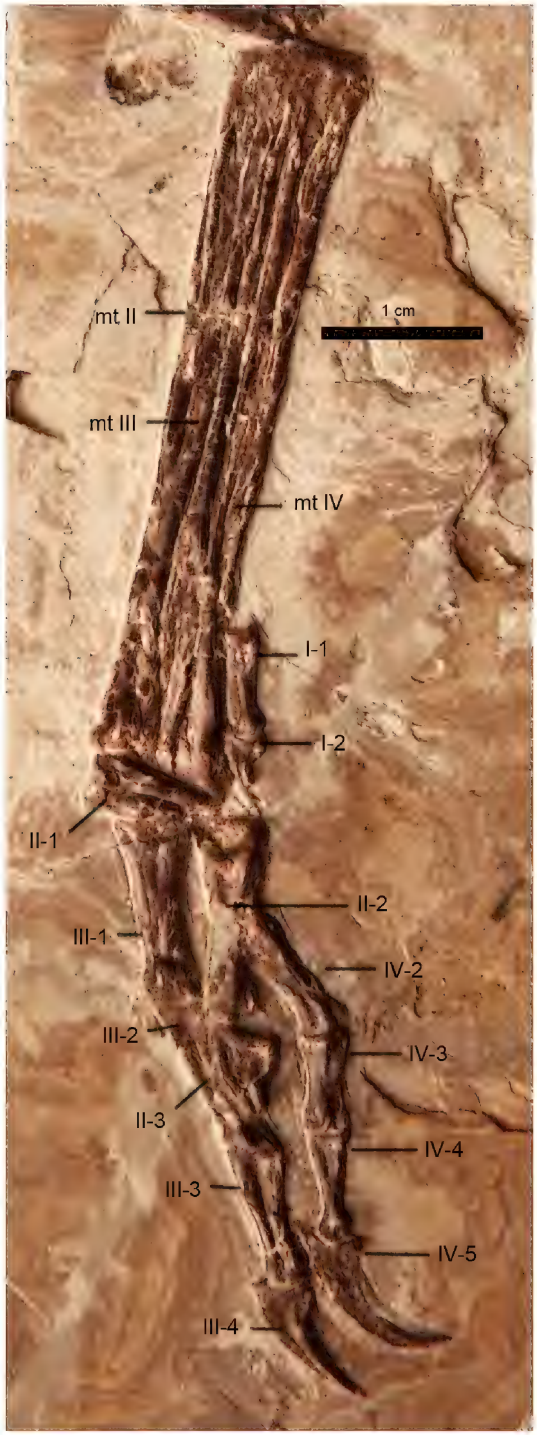

FIGURE 38. Right pes of BMNHC PH823.

metatarsal IV has a more expanded proximal end. Metatarsal III is exposed at the proximal end, but is not constricted significantly. On the right pes, metatarsal V is slender and splintlike, and is attached to metatarsal IV laterally. The morphology of the pes of BMNHC PH822 is similar to those of PKUP V1068 and BMNHC PH804 (figs. 37). The left pes is exposed in posterior view. Metatarsal III is not constricted in posterior view in BMNHC PH822.

In BMNHC PH804, pedal phalanx I-1 is less than 75% the length of phalanx II-1 (figs. 35, 36), which is the ancestral condition in most basal maniraptorans, and is in contrast to the elongate pedal phalanx I-1 of *Archaeopteryx* and more advanced avialans. An elongate pedal phalanx I-1 is also observed in the maniraptoran *Epidexipteryx* and *Balaur* (Zhang et al., 2008; Csiki et al., 2010; Brusatte et al., 2013). In BMNHC PH804, the right pedal phalanx IV-5 appears shorter than phalanx IV-4, but the left pedal phalanx IV-5 appears longer than phalanx IV-4 (table 1). This is mostly due to the incompleteness of the ungual phalanges making phalanx length difficult to determine in many cases. Ungual phalanges of BMNHC PH804 are not as curved as the manual ungual phalanges. Ungual phalanx II-3 is only slightly larger than phalanx III-4, and much larger than phalanx IV-5.

Plumage: Feathers associated with the postcranial skeletons are preserved in BMNHC PH804 and BMNHC PH822 as dark imprints (figs. 2, 3). Feather impressions in BMNHC PH804 are preserved in a better condition than in BMNHC PH822, but many of the feathers are not fully prepared and the tips are still buried in the matrix. The feather impressions of BMNHC PH822 are vague and incomplete. The distribution and the morphology of the feathers resemble other *Anchiornis* specimens closely (Hu et al., 2009; Li et al., 2010; Longrich et al., 2012)

The forelimbs of BMNHC PH804 and BMNHC PH822 are covered mostly with pennaceous feathers (figs. 2, 3, 39). In many cases, the rachis is observable, but the shape of the feather is uncertain in BMNHC PH804. The exact number and

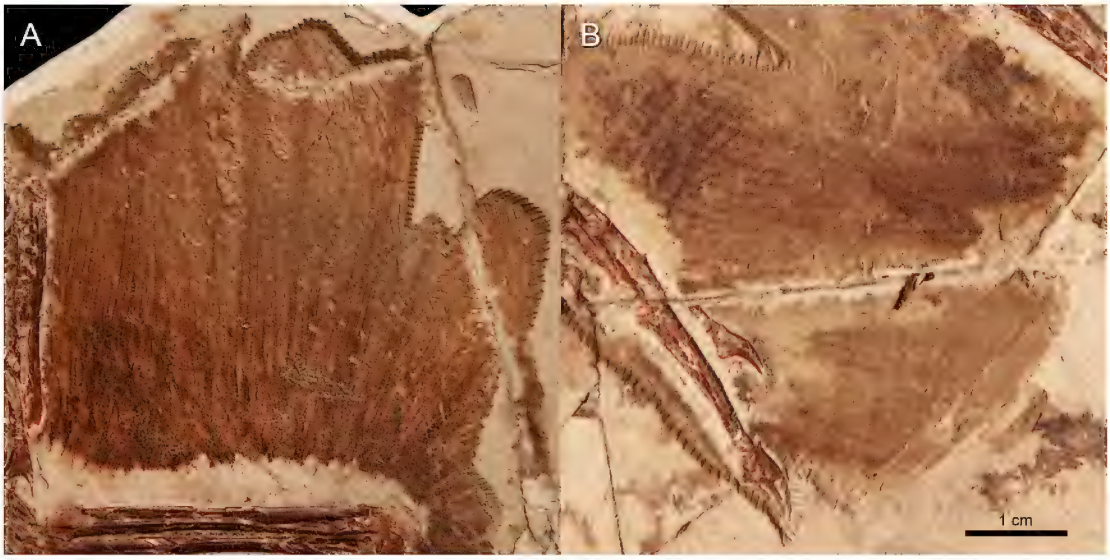

FIGURE 39. **A,** right wing of BMNHC PH804; **B,** left wing of BMNHC PH804.

shape of pennaceous feathers cannot be determined due to incomplete preparation and unideal preservation. Like *Archaeopteryx* and other *Anchiornis* specimens (Wellnhofer, 2009; Hu et al., 2009; Li et al., 2010; Longrich et al., 2012), the pennaceous feathers are likely more elongate approaching the distal end of the forelimb. In contract to *Microraptor* and derived avialans (Xu et al., 2003; Wellnhofer, 2009; Li et al., 2011), the pennaceous feathers are more symmetrical and shorter, probably lacking aerodynamic functions. On the right arm of BMNHC PH 804 (fig. 39), at least two tiers of pennaceous feathers could be recognized, which supports the stacking pattern observed in *Archaeopteryx* and *Anchiornis* as suggested by Longrich et al. (2012). Multiple layers of forelimb pennaceous feathers are also observed in BMNHC PH822.

Impressions of pennaceous feathers are associated with the hindlimbs of BMNHC PH804 and BMNHC PH822, which represents a typical condition in primitive paravians (fig. 2) (Xu et al., 2003). In contrast to *Microraptor* but like other *Anchiornis* specimens (Hu et al., 2009; Li et al., 2010, 2011), feather impressions are also observed associated with the pedal phalanges.

The proximal portion of the tail appears covered mostly by plumulaceous features, as no trace of rachides is observed, though some of the most proximal feathers appear to have a vague pennaceous outline (fig. 22). The length of the features decreases rapidly along the anterior one-third of the tail, and the shortened plumulaceous feathers are observable until at least the 15th caudal vertebra. A similar plumage configuration of the proximal portion of the tail is also observed in the referred specimen LPM-B00106 and other Jianchang paravians such as *Eosinopteryx* and *Aurornis* (Hu et al., 2009; Godefroit et al., 2013a, 2013b), but this pattern has not been preserved in *Microraptor* and *Caudipteryx*. In *Archaeopteryx*, the proximal portion of the tail appears associated with pennaceous feathers rather than plumulaceous feathers (Wellnhofer, 2009; Foth et al., 2014). The middle and distal portion of the tail is preserved with elongate pennaceous feathers that appear almost parallel to the caudal column, unlike the more expanded tail fan of *Archaeopteryx* (Wellnhofer, 2009). However, it is possible that this difference is preservational, as the orientation of the tail feathers could be changed postmortem.

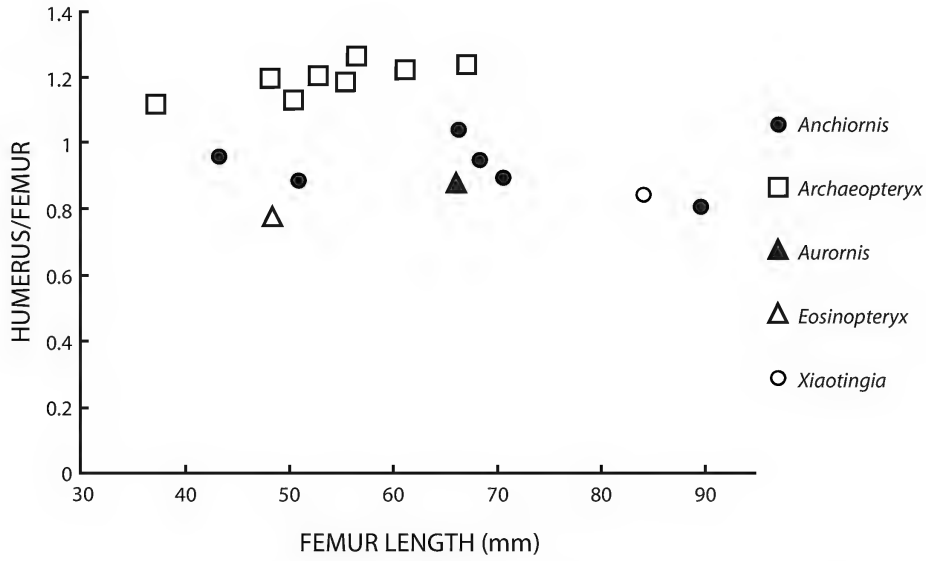

FIGURE 40. Distribution of humerus/femur ratio and femur length in *Anchiornis*, *Archaeopteryx*, *Aurornis*, *Eosinopteryx* and *Xiaotingia*.

DISCUSSION

Identity of New Specimens as *Anchiornis huxleyi* and Diagnosis of the Taxon

Anchiornis huxleyi was previously described based on the holotype IVPP V14378, and the referred specimens LPM-B00169 and BMNHC PH828. The holotype has a partial postcranial skeleton but is missing all the cranial bones (Xu et al., 2009). LPM-B00169 is nearly complete, but the cranium is shattered like many other *Anchiornis* specimens (Hu et al., 2009). BMNHC PH828 preserves a partial skull and partial postcranial skeleton (Li et al., 2010). Diagnostic features of *A. huxleyi* recognized by previous authors based on the fragmentary holotype IVPP V14378 include extreme shortness of the ischium and a sculpturing pattern of numerous small pits on the ventral surface of the coracoid (Xu et al., 2009).

All four new specimens (PKUP V1068, BMNHC PH804, BMNHC PH822, and BMNHC PH823) preserve complete skeletons, and PKUP V1068 also preserves an extraordinarily well-preserved skull. The extremely reduced ischium is present in BMNHC PH804, BMNHC PH822, BMNHC PH823, and the previously described LPM-B00169, while in PKUP V1068 the ischium is not exposed. The anterior/ventral surface of the coracoid of BMNHC PH822 is rugose, probably representing the sculpturing pattern of numerous small pits on the ventral surface of the coracoid of IVPP V14378. This slight difference is likely caused by the state of preservation.

All four new specimens resemble the holotype IVPP V14378 in the morphology of overlapping elements. In addition to the extreme shortness of the ischium, all reported *Anchiornis* specimens have the following postcranial features that are unseen or uncommon in other paravians: short and slender scapula that is about half the length of the humerus, short deltopectoral crest that is less than one-fourth the length of the humerus, straight ulna and straight radius, proportionally large radiale, significantly elongate manus, slightly curving metacarpal III, elongate tibiotarsus, fibula with an extremely expanded proximal end, and pedal phalanx II-1 subequal to or slightly shorter than phalanx

II-2. Major differences between the holotype and the new specimens are the position of the semilunate and the proportions, which are likely preservational artifacts and allometric variations (discussed below).

In addition, PKUP V1068, BMNHC PH804, BMNHC PH822, and BMNHC PH823 have a cranial morphology that is almost identical to the referred specimen LPM-B00169. These features include: straight nasal process of the premaxilla, external naris placed more posteriorly than the fourth premaxillary teeth, relatively short rostral ramus of the maxilla, enlarged maxillary fenestra, deep groove on the lateral surface of the dentary, and relatively small surangular foramen.

Although most of the listed features above are also observed in other Jianchang paravians such as *Xiaotingia*, *Eosinopteryx,* and *Aurornis*, some characters differ in those taxa and are discussed below.

These individual *Anchiornis huxleyi* specimens, IVPP V14378, LPM-B00169, PKUP V1068, BMNHC PH804, BMNHC PH822, and BMNHC PH823 are scored separately for a preliminary phylogenetic analysis. Minimum differences are present in the scorings, and therefore all new specimens can be safely referred to *Anchiornis huxleyi*. A complete phylogenetic analysis will be included in the future work with an expanded version of the latest TWiG (Theropod Working Group) data matrix (Brusatte et al., 2014). In this study, we solely use osteological features to discuss the taxonomy of *Anchiornis* and related taxa.

Based on our study of the new fossils in comparison with other specimens including the holotype, we here revise the diagnosis of *Anchiornis huxleyi* as follows: *Anchiornis huxleyi* is distinct from other paravians based on the combination of the following features: straight nasal process of the premaxilla, relatively short rostral ramus of the maxilla, ventrally displaced promaxillary fenestra of the maxilla, sheetlike posteroventral process of the dentary, rugose anterior/ventral surface of the coracoid, short deltopectoral crest no longer than one-fourth of the humeral shaft, straight ulna, and straight radius, extremely short ischium, and fibula with an extremely expanded proximal end as anteroposteriorly broad as the tibia. *Anchiornis huxleyi* differs from *Xiaotingia* in having a smaller surangular foramen, a short ischium less than one-fourth the length of the pubis, and metacarpal II much more robust than metacarpal III. *Anchiornis huxleyi* differs from *Eosinopteryx* in having more than 20 caudal vertebrae.

Affiliation of *Anchiornis huxleyi*

Affiliation to Maniraptora and Paraves

The morphology of *Anchiornis huxleyi* can be confidently assigned to the Maniraptora. Several synapomorphies of Maniraptora are present in *Anchiornis huxleyi*: broad triangular process along the lateral edge of the quadrate that contacts the squamosal and the quadratojugal; absence of the prefrontal, fused parietals, teeth constricted between the root and crown, reduced prezygapophyses on the distal caudal vertebrae, presence of a semilunate carpal; manual phalanx III-3 significantly elongate, and fibular shaft narrowing abruptly below the iliofibularis tubercle.

In many previous studies a monophyletic Paraves is recovered as a clade that includes Dromaeosauridae, Troodontidae, and Avialae (Gauthier, 1986; Sereno, 1997, Makovicky and Sues, 1998; Xu et al., 1999; Hwang et al., 2002; Makovicky et al., 2003; Xu and Norell, 2004; Makovicky et al., 2005; Novas and Pol, 2005; Norell et al., 2006; Turner et al., 2007, 2012; Hu et al., 2009; Senter et al., 2012; Brusatte et al., 2014; Foth et al., 2014; Lü and Brusatte, 2015). *Anchiornis huxleyi* can be referred to Paraves based on the following derived features: shallow maxilla and premaxilla below the external naris, T-shaped lacrimal; dentary symphyseal region in line with the main part of the buccal margin, chevrons anteriorly bifurcate on the distal part of the tail, nearly symmetric furcula, acromion margin of the scapula with a laterally everted anterior edge, coracoid inflected medially from the scapula, forming an L-shaped scapulocoracoid, humerus longer than

the scapula, ilium with the pubic peduncle much larger than the ischiadic peduncle, femur with a posterior trochanter, and the distal end of metatarsal III ginglymoid.

Within Paraves, the affiliation of *Anchiornis* is controversial (Xu et al., 2009, 2011; Hu et al., 2009; Turner et al., 2012; Senter et al., 2012; Foth et al., 2014). This confusion is caused mainly by the conservative morphology of basal paravians. However, careful examination of new specimens gives us better clue of the affiliation of *Anchiornis*.

Comparison with *Archaeopteryx*

Anchiornis huxleyi shares many features in common with *Archaeopteryx* that are not present in dromaeosaurids and troodontids. *Anchiornis* resembles *Archaeopteryx* in having: straight nasal process of the premaxilla, external naris posterior to all premaxillary teeth, fewer than 20 dentary teeth, absence of the coranoid eminence, absence of lateral exposure of the splenial, and absence of an external mandibular fenestra in lateral view. In the postcranial skeleton, *Anchiornis* shares the following features with *Archaeopteryx*: slightly bowed metacarpal III, pubic peduncle more ventrally expressed than the ischiadic peduncle, constricted base of the distally located obturator process, absence of a slit on the pubic apron, and proximal end of metatarsal III unconstricted. All of these features are found to be primitive for avialans, either as synapomorphies that are unique for avialans or synapomorphies of a more inclusive coelurosaurian clade that are secondarily lost in deinonychosaurians.

Anchiornis also shares the following features with *Archaeopteryx*: enlarged orbit, presence of a shallow premaxilla, presence of a promaxillary fenestra, enlarged maxillary fenestra, lacrimal with slender and subequal anterior and posterior processes, dorsal vertebrae with lateral concavities but not pneumatic foramina, scapula significantly shorter and slimmer than humerus, manual phalanx III-3 significantly longer than III-1 and III-2 combined, supraacetabular crest, and ischium with a distally located obturator process. However, these features are also present in many basal troodontids and dromaeosaurids and thus are primitive for Paraves.

Comparison with Troodontidae

Previous studies have assigned *Anchiornis* as a basal troodontid (Hu et al., 2009; Turner et al., 2012; Pei et al., 2014). Hu et al. (2009) suggested *Anchiornis* and others troodontids have the following features in common: large maxillary fenestra, labial surface of dentary bearing a distinct groove, closely packed premaxillary and dentary teeth in the symphyseal region, and dorsal vertebrae and anteriormost caudal vertebrae bearing relatively long and slender transverse processes. Hu et al. (2009) also suggested *Anchiornis* shares with *Mei* a large external naris extending posteriorly beyond and dorsal to the anterior border of antorbital fossa, a longitudinal groove along dorsomedial margin of the jugal, unserrated teeth, and a maxillary toothrow approaching the preorbital bar posteriorly. However, a large maxillary fenestra, a large external naris extending posteriorly beyond the anterior border of antorbital fossa, a longitudinal groove along dorsomedial margin of the jugal, unserrated teeth, and long transverse processes on dorsal vertebrae and anteriormost caudal vertebrae, are also present in *Archaeopteryx* and basal dromaeosaurids (Wellnhofer, 1974; Mayr et al., 2005; Makovicky et al., 2005; Foth et al., 2014; Pei et al., 2014). The primitive pennaraptoran *Epidexipteryx* also has closely packed premaxillary and dentary teeth in the symphyseal region (Zhang et al., 2008). The lateral groove on the dentary and maxillary toothrow approaching preorbital bar are observed in *Archaeopteryx* and other non-troodontid basal deinonychosaurians such as *Buitreraptor* (Wellnhofer, 1974; Makovicky et al., 2005). Thus, these features are all primitive to a more inclusive coelurosaurian clade.

In the phylogenetic analysis of Turner et al. (2012), three characters were recovered to support *Anchiornis* at the basalmost branch of Troodontidae, which include a dorsoventrally flattened internarial bar, the anteroventrally

inclined quadrate and a subarctometatarsalian pes. In scoring based on a new *Archaeopteryx* specimen (Foth et al., 2014), the internarial bar of *Archaeopteryx* is scored as dorsoventrally flat as in troodontids like *Sinovenator*, *Byronosaurus,* and *Zanabazar*, and a dorsoventrally flat internarial bar is also observed in the dromaeosaurid *Microraptor* (Pei et al., 2014), so this feature is no longer restricted to Troodontidae. Both dorsoventrally flat (e.g., Eichstätt and Thermopolis specimens) and rodlike (e.g., Solnhofen specimen) internarial bars are actually observed in *Archaeopteryx*. The anteroventrally inclined quadrate is also observed in *Archaeopteryx* and more basal taxa such as *Sinosauropteryx* and *Ornithomimus* (Ji and Ji, 1996; Wellnhofer, 2009; Rauhut, 2014), and thus it is a synapomorphy of a larger clade. The arctometatarsalian pes of *Anchiornis* is dubious, and new specimens revealed the pes of *Anchiornis* resembles more the normal pedal configuration of *Archaeopteyrx* than it does the arctometatarsalian pes of *Microraptor* and *Sinovenator*. As discussed above, these three characters no longer adequately support *Anchiornis* as a member of Troodontidae.

As a Jurassic basal paravian, *Anchiornis huxleyi* differs from troodontids in several features. These features include: posteriorly tapering ventral ramus of the maxilla, elongation of the forelimb, middle and posterior maxillary teeth sparsely spaced, fewer than 20 dentary teeth, presence of a basisphenoid recess, wide and dorsoventrally low foramen magnum, transition of elongate caudal vertebrae occurring before the 10th caudal vertebra and symmetric metatarsus. These features are primitive for paravians and are found in basal dromaeosaurids and/or basal avialans, but absent in troodontids.

Comparison with Deinonychosauria

Because *Anchiornis* displays many primitive paravians features that are present in both troodontids and the basal avialan *Archaeopteryx*, it is necessary to look at derived features of Deinonychosauria in order to distinguish *Anchiornis* from Troodontidae. *Anchiornis* does not have a lateral exposure of the splenial and also lacks a specialized raptorial digit II, which differentiates it from deinonychosaurians.

Some features that are regarded as derived characters in deinonychosaurians, such as a subarctometatarsalian pes and a raptorial pedal digit II, were considered to be present in *Anchiornis* and used as evidence for a troodontid affiliation of this taxon (Hu et al., 2009). However, careful examination of *Anchiornis* specimens indicates *Anchiornis* resembles *Archaeopteryx* in these pedal characters.

The pes of *Anchiornis* is reported as subarctometatarsalian (Xu et al., 2009; Hu et al., 2009). But close examination and comparison of new *Anchiornis* specimens indicate that the proximal end of metatarsal III is not significantly constricted. Instead, the proximal end of metatarsal III has a subequal width as metatarsals II and IV in anterior view, which resembles *Archaeopteryx* and most nontroodontid theropods, but different from the subarctometatarsus of basal troodontids (e.g. *Sinovenator* and *Mei*) and the type specimen of *Sinornithosaurus* and *Microraptor*, where the proximal end of metatarsal III is significantly reduced in width in anterior view compared to metatarsal II and metatarsal IV (Xu et al., 1999, 2000, 2002; Xu, 2002; Xu and Norell, 2004). *Anchiornis* was also reported to have a deinonychosaurian-like pedal digit II (Xu et al., 2009; Hu et al., 2009). Careful examination of more specimens of *Anchiornis* indicates that pedal digit II of these specimens lacks the typical specialized raptorial condition of deinonychosaurians. In *Anchiornis*, pedal phalanx II-2 is not reduced in length and lacks a well-developed ventral heel or a constriction at midshaft, which is different from deinonychosaurians (Gauthier, 1986; Turner et al., 2012). Ungual phalange II-3 of *Anchiornis* is only slightly larger than other pedal ungual phalanges, not as distinctly enlarged as in deinonychosaurians. Although the pedal digit II of *Anchiornis* is more derived than the configuration of basal maniraptoriforms (such as ornithomimosaurians, alva-

rezsaurids, and oviraptorosaurians), it still exhibits the primitive features (as mentioned above) of paravians that is also observed in *Archaeopteryx* (see Turner et al., 2012). As a contrast in deinonychosaurians, even the basal members of each lineage, such as *Mahakala* and *Sinovenator* have highly modified and hyperextensible pedal digit II that is different from *Anchiornis* and *Archaeopteryx* (Xu et al., 2002; Turner et al., 2007, 2011, 2012).

We consider *Anchiornis huxleyi* as a basal avialan based on derived characters it shares with other avialans (Xu et al., 2009; Godefroit et al., 2013a; Foth et al., 2014), such as a straight nasal process of the premaxilla and the absence of an external mandibular fenestra in lateral view. *Anchiornis* also lacks typical deinonychosaurian synapomorphies such as lateral exposure of the splenial, and a specialized raptorial pedal digit II, which differentiates *Anchiornis* from deinonychosaurians.

Variation within Specimens of *Anchiornis huxleyi*

Though all reported specimens of *Anchiornis* have significant similarities in morphology, some variation does exist. PKUP V1068 is the largest (based on femoral length) among the four new specimens. It differs from the other specimens in having a different number of caudal vertebrae. In PKUP V1068, only 22 caudal vertebrae are present. In contrast, 31 to 32 caudal vertebrae are counted in the holotype, BMNHC PH804, BMNHC PH822, and BMNHC PH823. However, the first few exposed caudal vertebrae of PKUP V1068 are elongate and longer than the last dorsal vertebra, while in other *Anchiornis* specimens, the anterior caudal vertebrae are relatively reduced and significantly shorter than the last dorsal vertebra (fig. 17). The first few exposed caudal vertebrae of PKUP V1068 also lack the prominent transverse processes that are present on the anteriormost caudal vertebrae in other specimens (figs. 21–C, 22). In PKUP V1068, the 6th exposed caudal vertebra reaches the maximum centrum length (fig. 21A), while in other specimens the longest centrum is at ~12th–14th caudal vertebrae (figs. 21B, C, 22). All evidence indicates that the proximalmost caudal vertebrae of PKUP V1068 are either not exposed or missing during the severe twist at the pelvic region when this specimen was buried. The actual number of caudal vertebrae in PKUP V1068 should be much greater than 22, and likely close to 30.

The position of the semilunate varies in the reported *Anchiornis* specimens. In the holotype IVPP V14378, the semilunate is small and mainly covers the proximal ends of metacarpals II and III; in LPM-B00169, it covers the proximal ends of all three metacarpals (Xu et al., 2009; Hu et al., 2009). Based on observations of IVPP V14378 and LPM-B00169, Hu et al. (2009) inferred that this difference might be a preservational artifact, and the semilunate should have contacted all metacarpals in these specimens. In PKUP V1068, the left semilunate centers on both metacarpal I and metacarpal II, and has a medial process that contacts metacarpal III as in LPM-B100169 (fig. 28). The right semilunate of PKUP V1068 centers on metacarpal II and possibly has a slight contact with both metacarpals I and III (fig. 29). In both wrists of BMNHC PH804 and the right wrist of BMNHC PH822, the semilunate contacts metacarpals I and II, with no contact with metacarpal III (figs. 25, 26, 30). But this observation may be influenced by the angle of observation. In BMNHC PH804 and BMNHC PH822, the manus is laterally preserved, and thus metacarpal III is laterally obscured by metacarpals I and II. The preservation state of the wrists of PKUP V1068, BMNHC PH804, and BMNHC PH822 supports the interpretation of Hu et al. (2009) that the semilunate has a possible contact with all three metacarpals in *Anchiornis huxleyi*. If this is the case, the wrist structure of *Anchiornis* resembles some derived dromaeosaurids, such as *Velociraptor* and *Deinonychus* (Ostrom, 1969; Gishlick, 2001).

Proportional variations have been reported in *Anchiornis* specimens (Xu et al., 2009; Hu et al.,

2009). For example, IVPP V14378, PKUP V1068, BMNHC PH804, BMNHC PH822, and BMNHC PH823 have a femur that is longer than the humerus. However, LPM-B00169 is reported to have a slightly longer humerus than femur (femur/humerus ratio = 0.95) (Hu et al., 2009).

IVPP V14378, BMNHC PH804, BMNHC PH822, and BMNHC PH823 have a femur/humerus ratio between 1.05 and 1.15, but the femur of PKUP V1068 is relatively longer (femur/humerus ratio = 1.24). The hindlimb of PKUP V1068 is slightly elongate compared with other reported *Anchiornis* specimens. A similar pattern is observed in the size-comparable paravian *Archaeopteryx lithographica* (fig. 40). The Berlin *Archaeopteryx* specimen has a skull size close to that of the Thermopolis *Archaeopteryx* specimen, but their humerus/femur ratios are 1.13 and 1.21 respectively (Mayr et al., 2007). Thus, the proportional differences of these *Anchiornis* specimens could be inferred as intraspecies variations as in *Archaeopteryx lithographica.* This agrees with the interpretation that the slight elongation of hindlimbs of PKUP V1068 is an intraspecies variation and possibly due to the allometric growth. The skull of PKUP V1068 was compressed anteroposteriorly during preservation, as evidenced by the displacement of the maxilla-lacrimal contact and the anteroposteriorly compressed lower temporal fenestra (fig. 5). Therefore, the actual skull size of PKUP V1068 should be longer than it seems and is the largest among the reported *Anchiornis* specimens, even though the skull of PKUP V1068 appears very close in length to that of BMNHC PH822 (table 1).

Comparisons with *Pedopenna*, *Xiaotingia*, *Eosinopteryx*, and *Aurornis*

Pedopenna daohugouensis (Xu and Zhang, 2005) is a Jurassic paravian reported in 2005 based on hindlimbs from the Daohugou area of the Yanliao Biota. *Pedopenna* differs from *Anchiornis* from the proportions of pedal phalanges (Xu and Zhang, 2005). The morphology of the hindlimb of *Pedopenna* is conservative, and is very similar to the Jianchang paravians. However, the type specimen (which is also the only specimen) of *Pedopenna* is very poorly preserved and prevents further comparison.

Three Jurassic paravians, *Xiaotingia*, *Eosinopteryx,* and *Aurornis,* have been reported from the Jianchang area following the discovery of *Anchiornis huxleyi* (Xu et al., 2011; Godefroit et al., 2013a, 2013b). All of those other taxa are based on single specimens. *Xiaotingia* was reported in 2011, based on a specimen with a complete skull and a partial postcranial skeleton, missing the tail, partial pectoral girdle, and distal hindlimb. *Eosinopteryx* and *Aurornis* were reported in 2013, both with complete cranial and postcranial skeletons. However, several bones of these three specimens are shattered and split like many other western Liaoning dinosaurs, so they provide only limited anatomical information.

These Jianchang paravians (*Xiaotingia*, *Eosinopteryx,* and *Aurornis*) closely resemble *Anchiornis huxleyi* in a number of characters: straight nasal process of the premaxilla, posteriorly placed external naris, relatively short rostral ramus of the maxilla, ventrally displaced promaxillary fenestra, dentary with a distinct lateral groove, sheetlike posteroventral process of the dentary, mandible that is significantly deeper posteriorly than anteriorly, short deltopectoral crest, straight ulna and radius, and extremely expanded proximal end of the fibula. An extremely short ischium is also shared by *Anchiornis*, *Eosinopteryx,* and *Aurornis.* All recently reported paravians from Jianchang County likely form a monophyletic group based on their anatomical similarities (also see Foth et al., 2014).

In the original diagnoses for *Xiaotingia*, it differs from *Anchiornis* in having the following unique features: maxillary posterior ramus has a depth at midlength exceeding that of the dentary; surangular has a small lateral exposure and forms a wide, flat dorsal surface over the posterior part of the mandible; large surangular foramen extends over more than 6% of the total mandibular length; posterior end of the mandible is blunt and dorsoventrally expanded; anteriormost caudal centra are less than half as

long as the posterior dorsal centra; metacarpal III is more robust than metacarpals I and II; and manual phalanx II-2 is longer than metacarpal II (Xu et al., 2011). In *Anchiornis*, the subantorbital-fenestra portion of the maxilla (to be clear, the posterior ramus [ventral ramus] of the maxilla is actually thin, but a distance exists between the ventral ramus and the antorbital fenestra in all specimens of *Anchiornis*) is dorsoventrally deep and the posterior end of the mandible is also dorsoventrally expanded, as in *Xiaotingia*. The proportional differences of the caudal vertebrae, an elongate surangular foramen, and manual phalanx II-2 longer than metacarpal II are likely a result of allometric variation. However, other diagnostic features of *Xiaotingia*, such as the surangular with little lateral exposure, forming a wide dorsal surface over the posterior part of the mandible, and a much more robust metacarpal III, are not observed in any reported *Anchiornis* specimens. *Xiaotingia* also differs from other Jianchang paravians in having a proportionally longer ischium.

Eosinopteryx is diagnosed by: short snout; lacrimal with a longer posterior process; short tail of 20 caudal vertebrae; chevrons reduced to small rodlike elements below the proximal 8th or 9th caudals; ilium with a proportionally long, low, and distally tapering postacetabular process; pedal unguals shorter than corresponding penultimate phalanges; and absence of rectrices and feathers on the metatarsus (Godefroit et al., 2013a). In this study we find not all these features are diagnostic. The snout of YFGP-T5197 (type specimen of *Eosinopteryx brevipenna*) is broken and incomplete, and thus cannot be used for comparison. Moreover, the anteroposterior length of the preorbital portion of the skull is about 1.5–2 times that of the orbit, which is the same as in *Anchiornis*. The lacrimal of BMNHC PH804 has both long anterior and posterior processes, but both processes are extremely slender and easy to break, so the longer posterior process of the lacrimal is not a reliable diagnostic feature of *Eosinopteryx*. Reduced chevrons below the proximal 8th or 9th caudal vertebrae are observed in other *Anchiornis* specimens, such as BMNHC PH804 and BMNHC PH822. *Anchiornis* specimens have variation in proportions of pedal phalanges, even within the same specimen, such as in BMNHC PH804 (see above). A long and low posterior (= postacetabular) process of the ilium is also present in *Anchiornis* (e.g., IVPP V14378, BMNHC PH804, BMNHC PH822, and BMNHC PH823). The absence of rectrices and feathers on the metatarsus is possibly a preservational artifact, as many *Anchiornis* specimens only have feathers associated with few bones instead of the entire body. The characters mentioned above cannot be regarded as solid diagnosis to distinguish *Eosinopteryx* from *Anchiornis*. However, a short tail does differentiate *Eosinopteryx* from *Anchiornis*. Normally more than 30 caudal vertebrae are preserved in *Anchiornis*. Even if only 22 caudal vertebrae are observed in PKUP V1068, it clearly does not represent the life condition of that specimen. Moreover, the 12th–14th caudal vertebrae reach the maximum length in *Eosinopteryx*, as in most *Anchiornis* specimens, while the 6th exposed caudal vertebra reaches the maximum length in PKUP V1068. The morphology of *Eosinopteryx* is mostly identical to that of *Anchiornis*, except for the short length of the tail in the former. We regard *Eosinopteryx* as a valid taxon, but firsthand examination of the specimen is necessary to further confirm this conclusion.

As mentioned by Godefroit et al. (2013b), *Aurornis xui* (YFGP-T5198) differs from *Anchiornis huxleyi* in having an elongate subnarial process of the premaxilla, an elongate posterior process of the lacrimal, a relatively shorter and more gracile humerus compared to the femur, a postacetabular process that is quadrangular in lateral view, the presence of a hooked ischium, an elongate metatarsal I that is not reduced to a splint, and the shorter penultimate phalanges of the pedal digits (Godefroit et al., 2013b: supplementary information). However, these features are inadequate to differentiate *Aurornis* from *Anchiornis* as a distinct new taxon. Many cranial bones of YFGP-T5198 are shattered, and the presumed subnarial process is not confluent with

the remainder of the premaxilla (Godefroit et al., 2013b: fig. 2a), and thus likely a misidentification. The elongate piece of bone exposed between the shattered nasal and maxilla is possibly the vomer or the ventral ramus of the adjacent maxilla, but this assertion requires further examination of the specimen to validate it. BMNHC PH804 also has an elongate posterior process of the lacrimal as in YFGP-T5198. Although the long posterior process of the lacrimal is not observed in all *Anchiornis* specimens, it is likely a preservational artifact, since this process is extremely slender and difficult to preserve. The humerus of YFGP-T5198 is relatively shorter and more slender than the femur, with a femur/humerus ratio of 1.13, but it is within the range that is observed in other *Anchiornis* specimens (discussed above). The posterior (= postacetabular) process of the right ilium of YFGP-T5198 is more squared than in other *Anchiornis*, but the left posterior (= postacetabular) process of YFGP-T5198 is dorsoventrally shallow and has a posteroventrally sloping dorsal edge as in other *Anchiornis* specimens (e.g., IVPP V14378, LPM-B00169, BMNHC PH804, BMNHC PH822, and BMNHC PH823). The elongation of metatarsal I in *Aurornis* is also likely a preservational artifact, as no complete metatarsal I is preserved/exposed in any reported *Anchiornis* specimens. *Anchiornis* also shows variation in proportions of pedal phalanges, even within the same specimen (BMNHC PH804), and thus the shorter penultimate phalanges of the pedal digits also cannot differentiate *Aurornis* from *Anchiornis*.

SUMMARY

Four new specimens of *Anchiornis huxleyi* reveal new osteological details of this important paravian taxon. *Anchiornis huxleyi* exhibits many conservative paravian features, and closely resembles *Archaeopteryx* and other paravians from Jianchang County, such as *Xiaotingia* and *Eosinopteryx*. *Aurornis xui*, however, is likely a junior synonym of *Anchiornis huxleyi*.

Anchiornis huxleyi shares derived features with avialans, such as a straight nasal process of the premaxilla, and the absence of an external mandibular fenestra in lateral view. *Anchiornis* also lacks derived deinonychosaurian characteristics, including a laterally exposed splenial and a specialized raptorial pedal digit II. *Anchiornis* appears to be more closely related to avialans than deinonychosaurians or troodontids, based on morphological comparisons and identification of potential synapomorphies in this analysis.

ACKNOWLEDGMENTS

We are grateful to Xu Xing and Hu Dongyu for access to other paravian specimens including the holotype of *Anchiornis huxleyi*. We also thank Jia Jia, Zeng Zhaohui, and Liu Di for arranging the lab in Beijing, Mick Ellison for photographing the specimens and preparing the figures. We thank John Flynn, Meng Jin, Peter Makovicky, and Alan Turner for reading the manuscript and providing useful advice. This project was supported by the Division of Paleontology at the American Museum of Natural History, Columbia University, and the Jurassic Foundation.

REFERENCES

Agnolín, F.L., and F.E. Novas. 2013. Avian ancestors: a review of the phylogenetic relationships of the theropods Unenlagiidae, Microraptoria, *Anchiornis*, and Scansoriopterygidae. SpringerBriefs in Earth System Sciences 99.

Alonso, P.D., A.C. Milner, R.A. Ketcham, M.J. Cookson, and T.B. Rowe. 2004. The avian nature of the brain and inner ear of *Archaeopteryx*. Nature 430: 666–669.

Averianov, A.O., and H.D. Sues. 2007. A new troodontid (Dinosauria: Theropoda) from the Cenomanian of Uzbekistan, with a review of troodontid records from the territories of the former Soviet Union. Journal of Vertebrate Paleontology 27 (1): 87–98.

Balanoff, A.M., and M.A. Norell. 2012. Osteology of *Khaan mckennai* (Oviraptorosauria: Theropoda). Bulletin of the American Museum of Natural History 372: 1–77.

Barsbold, R., and H. Osmólska. 1999. The skull of *Velociraptor* (Theropoda) from the Late Cretaceous of Mongolia. Acta Palaeontologica Polonica 44 (2): 189–219.

Brusatte, S.L., et al. 2013. The osteology of *Balaur bondoc*, an island-dwelling dromaeosaurid (Dinosauria: Theropoda) from the Late Cretaceous of Romania. American Museum Novitates 374: 1–100.

Brusatte, S.L., G.T. Lloyd, S.C. Wang, and M.A. Norell. 2014. Gradual assembly of avian body plan culminated in rapid rates of evolution across the dinosaur-bird transition. Current Biology 24: 2386–2392.

Burnham, D.A., et al. 2000. Remarkable new birdlike dinosaur (Theropoda: Maniraptora) from the Upper Cretaceous of Montana. University of Kansas Paleontological Contributions (new series) 13: 1–14.

Chiappe, L.M., S. Ji, Q. Ji, and M.A. Norell. 1999. Anatomy and systematics of the Confuciusornithidae (Theropoda: Aves) from the Late Mesozoic of northeastern China. Bulletin of the American Museum of Natural History 242: 1–89.

Cohen, K.M., S.C. Finney, P.L. Gibbard, and J.-X. Fan. 2013. The ICS International Chronostratigraphic Chart. Episodes 36: 199–204.

Csiki, Z., M. Vremir, S.L. Brusatte, and M.A. Norell. 2010. An aberrant island-dwelling theropod dinosaur from the Late Cretaceous of Romania. Proceedings of the National Academy of Sciences of the United States of America 107 (35): 15357–15361.

Currie, P.J. 1995. New information on the anatomy and relationships of *Dromaeosaurus albertensis* (Dinosauria: Theropoda). Journal of Vertebrate Paleontology 15: 576–591.

Currie, P.J., and Z. Dong. 2001. New information on Cretaceous troodontids (Dinosauria, Theropoda) from the People's Republic of China. Canadian Journal of Earth Sciences 38: 1753–1766.

Currie, P.J., and X. Zhao. 1993. A new troodontid (Dinosauria, Theropoda) braincase from the Dinosaur Park Formation (Campanian) of Alberta. Canadian Journal of Earth Sciences 30: 2231–2247.

Elżanowski, A. 2001. A new genus and species for the largest specimen of *Archaeopteryx*. Acta Palaeontologica Polonica 46: 519–532.

Elzanowski, A., and P. Wellnhofer. 1996. Cranial morphology of *Archaeopteryx*: evidence from the seventh skeleton. Journal of Vertebrate Paleontology 16: 81–94.

Forster, C.A., S.D. Sampson, L.M. Chiappe, and D.W. Krause. 1998. The theropod ancestry of birds: new evidence from the Late Cretaceous of Madagascar. Science 279: 1915–1919.

Foth, C., H. Tischlinger, and O.W.M. Rauhut. 2014. New specimen of *Archaeopteryx* provides insights into the evolution of pennaceous feathers. Nature 511: 79–82.

Gao, C., E.M. Morschhauser, D.J. Varricchio, J. Liu, and B. Zhao. 2012. A second soundly sleeping dragon: new anatomical details of the Chinese troodontid *Mei long* with implications for phylogeny and taphonomy. PLoS ONE 7 (9): e45203.

Gao, K.-Q., and N.H. Shubin. 2012. Late Jurassic salamandroid from western Liaoning, China. Proceedings of the National Academy of Sciences of the United States of America 109 (15): 5767–5772.

Gauthier, J.A. 1986. Saurischian monophyly and the origin of birds. *In* K. Padian (editor), The origin of birds and evolution of flight. 1–55. San Francisco: California Academy of Sciences Memoir.

Gishlick, A.D. 2001. The function of the manus and forelimb of *Deinonychus antirrhopus* and its importance for the origin of avian flight. *In* J.A. Gauthier and L.F. Gall (editors), New perspectives on the origin and early evolution of birds: 301–318. New Heaven: Peabody Museum of Natural History, Yale University.

Godefroit, P., A. Cau, Hu D.-Y., F. Escuillie, W. Wu, and G. Dyke. 2013a. Reduced plumage and flight ability of a new paravian theropod from China. Nature Communications 4: 1394.

Godefroit, P., A. Cau, Hu D.-Y., F. Escuillie, W. Wu, and G. Dyke. 2013b. A Jurassic avialan dinosaur from China resolves the early phylogenetic history of birds. Nature 498: 359 –362.

Hu, D., L. Hou, L. Zhang, and X. Xu. 2009. A pre-*Archaeopteryx* troodontid theropod from China with long feathers on the metatarsal. Nature 461: 640–643.

Hwang, S.H., M.A. Norell, Q. Ji, and K.-Q. Gao. 2002. New specimens of *Microraptor zhaoianus* (Theropoda, Dromaeosauridae) from northeastern China. American Museum Novitates 3381: 1–44.

Ji, Q., and S. Ji. 1996. On discovery of the earliest bird fossil in China and the origin of birds. Chinese Geology 10: 30–33.

Ji, Q., and C. Yuan. 2002. Discovery of two kinds of protofeathered pterosaurs in the Mesozoic Daohugou Biota in the Ningcheng region and its stratigraphic and biologic significances. Geological Review 48: 221–224.

Ji, Q., P.J. Currie, M.A. Norell, and S. Ji. 1998. Two feathered dinosaurs from northeastern China. Nature 393: 753–761.

Ji, Q., et al. 2005. First avialan bird from China (*Jinfengopteryx elegans* gen. et sp. nov.). Geological Bulletin of China, 24 (3): 197–205.

Ji, S., and Q. Ji. 2007. *Jinfengopteryx* compared to *Archaeopteryx*, with comments on the mosaic evolution of long-tailed avialan birds. Acta Geologica Sinica (English edition) 81 (3): 337–343.

Li, Q.-G., et al. 2010. Plumage color patterns of an extinct dinosaur. Science. 327 (5971): 1369–1372.

Longrich, N.R., J. Vinther, Q. Meng, Q. Li, and A.P. Russell. 2012. Primitive wing feather arrangement in *Archaeopteryx lithographica* and *Anchiornis huxleyi*. Current Biology 22: 1–6.

Luo, Z., P. Chen, G. Li, and M. Chen. 2007a. A new eutriconodont mammal and evolutionary development in early mammals. Nature 446: 288–293.

Luo, Z., Q. Ji and C. Yuan. 2007b. Convergent dental adaptations in pseudotribosphenic and tribosphenic mammals. Nature 450: 93–97.

Luo, Z., C. Yuan, Q. Meng, and Q. Ji. 2011. A Jurassic eutherian mammal and divergence of marsupials and placentals. Nature 476: 442–445.

Lü J., and S.L. Brusatte. 2015. A large, short-armed, winged dromaeosaurid (Dinosauria: Theropoda) from the Early Cretaceous of China and its implications for feather evolution. Scientific Reports 5: 11775.

Lü, J., D.M. Unwin, X. Jin, Y. Liu, and Q. Ji, 2009. Evidence for modular evolution in a long-tailed pterosaur with a pterodactyloid skull. Proceedings of the Royal Society of London Series B 227: 383–389.

Lü, J., et al. 2010. A new troodontid theropod from the Late Cretaceous of central China, and the radiation of Asian troodontids. Acta Palaeontologica Polonica 55: 381–388.

Makovicky, P.J., and M.A. Norell. 2004. Troodontidae. *In* D.B. Weishampel, P. Dodson, and H. Osmólska (editors), The Dinosauria: 184–195. Berkeley: University of California Press.

Makovicky, P.J., and H.D. Sues. 1998. Anatomy and phylogenetic relationships of the theropod dinosaur *Microvenator celer* from the Lower Cretaceous of Montana. American Museum Novitates 3240: 1–27.

Makovicky, P.J., M.A. Norell, J.M. Clark, and T.E. Rowe. 2003. Osteology and relationships of *Byronosaurus jaffei* (Theropoda: Troodontidae). American Museum Novitates 3402: 1–32.

Makovicky, P.J., Y. Kobayashi, and P.J. Currie. 2004. Ornithomimosauria. *In* D.B. Weishampel, P. Dodson, and H. Osmólska (editors), The Dinosauria, 2nd ed.: 137–150. Berkeley: University of California Press.

Makovicky, P.J., S. Apesteguía, and F.L. Agnolín. 2005. The earliest dromaeosaurid theropod from South America. Nature 437: 1007–1011.

Mayr, G., B. Pohl, and D.S. Peters. 2005. A well-preserved *Archaeopteryx* specimen with theropod features. Science 310: 1483–1486.

Mayr, G., B. Phol, S. Hartman, and D.S. Peters. 2007. The 10th skeletal specimen of *Archaeopteryx*. Zoological Journal of the Linnean Society 149: 97–116.

Meng, J., Y. Hu, Y. Wang, X. Wang, and C. Li. 2006. A Mesozoic gliding mammal from northeastern China. Nature 444: 889–893.

Nesbitt, S.J., A.H. Turner, M. Spaulding, J.L. Conrad, and M.A. Norell. 2009. The theropod furcula. Journal of Morphology 270: 856–879.

Norell, M.A., and P.J. Makovicky. 1997. Important features of the dromaeosaur skeleton: information from a new specimen. American Museum Novitates 3215: 1–28.

Norell, M.A., and P.J. Makovicky. 1999. Important features of the dromaeosaur skeleton II: information from newly collected specimens of *Velociraptor mongoliensis*. American Museum Novitates 3282: 1–45.

Norell, M.A., and P.J. Makovicky. 2004. Dromaeosauridae. *In* D.B. Weishampel, P. Dodson, and H. Osmólska (editors), The Dinosauria: 196–209. Berkeley: University of California Press.

Norell, M.A., J.M. Clark, and P.J. Makovicky. 2001. Phylogenetic relationships among coelurosaurian theropods. *In* J. Gauthier and L.F. Gall (editors), New perspectives on the origin and early evolution of birds: proceedings of the international symposium in honor of John H. Ostrom: 49–67. New Haven: Peabody Museum of Natural History.

Norell, M.A., P.J. Makovicky, and J.M. Clark. 2004. The braincase of *Velociraptor*. *In* P.J. Currie, E.B. Koppelhaus, and M.B. Shugar (editors). Feathered dragons: studies on the transition from dinosaurs to birds. Bloomington: Indiana University Press.

Norell, M.A., et al. 2006. A new dromaeosaurid theropod from Ukhaa Tolgod (Ömnögov, Mongolia). American Museum Novitates 3545: 1–51.

Norell, M.A., et al. 2009. A review of the Mongolian Cretaceous dinosaur *Saurornithoides* (Troodontidae: Theropoda). American Museum Novitates 3654: 1–63.

Novas, F.E., and D. Pol. 2005. New evidence on deinonychosaurian dinosaurs from the Late Cretaceous of Patagonia. Nature 433: 858–861.

Novas, F.E., and P.F. Puerta. 1997. New evidence concerning avian origins from the Late Cretaceous of Patagonia. Nature 387: 390–392.

O'Connor, P.M. and C.A. Forster. 2010. A Late Cretaceous (Maastrichtian) Avifauna from the Maevarano Formation, Madagascar. Journal of Vertebrate Paleontology 30 (4): 1178–1201.

Osborn, H.F. 1924. Three new Theropoda, Protoceratops zone, central Mongolia. American Museum Novitates 144: 1–12.

Ostrom, J.H. 1969. Osteology of *Deinonychus antirrhopus*, an unusual theropod from the Lower Cretaceous of Montana. Bulletin of the Peabody Museum of Natural History 30: 1–165.

Pei, R., Q. Li, Q. Meng, K. Gao, and M.A. Norell. 2014. A new specimen of *Microraptor* (Theropoda: Dromaeosauridae) from the Lower Cretaceous of western Liaoning, China. American Museum Novitates 3821: 1–28.

Perle, A., M.A. Norell, and J.Clark. 1999. A new maniraptoran theropod – *Achillobator giganticus* (Dromaeosauridae) – from the Upper Cretaceous of Burkhant, Mongolia. Contributions of the Mongolian-American Paleontological Project 101: 1–105.

Rauhut, O.W.M. 2014. New observations on the skull of *Archaeopteryx*. Paläontologische Zeitschrift 88: 211–221.

Ren, D., C.K. Shih, T. Gao, Y. Yao, and Y. Zhao. 2010. Silent stories: insect fossil treasures from dinosaur era of the northeastern China. Beijing: Science Press.

Senter, P., R. Barsbold, B. Britt, and D.A. Burnham. 2004. Systematics and evolution of Dromaeosauridae (Dinosauria, Theropoda). Bulletin of the Gunma Museum of Natural History 8: 1–20.

Senter, P., J.I. Kirkland, D.D. DeBlieux, S. Madsen, N. Toth. 2012. New dromaeosaurids (Dinosauria: Theropoda) from the Lower Cretaceous of Utah, and the evolution of the dromaeosaurid tail. PLoS ONE 7 (5): e36790.

Sereno, P.C. 1997. The origin and evolution of dinosaurs. Annual Review of Earth and Planetary Sciences 25: 435–489.

Sullivan, C., et al. 2014. The vertebrates of the Jurassic Daohugou Biota of northeastern China. Journal of Vertebrate Paleontology 2: 243–280.

Tsuihiji, T., et al. 2014. An exquisitely preserved troodontid theropod with new information from the palatal structure from the Upper Cretaceous of Mongolia. Naturwissenschaften 101: 131. [doi 10.1007/s00114-014-1143-9]

Turner, A.H., D. Pol., J.A. Clarke, G. Erickson, and M.A. Norell. 2007. A basal dromaeosaurid and size evolution preceding avian flight. Science 317: 1378–1381.

Turner, A.H., D. Pol, and M.A. Norell. 2011. Anatomy of *Mahakala omnogovae* (Theropoda: Dromaeosauridae), Tögrögiin Shiree, Mongolia. American Museum Novitates 3722: 1–66.

Turner, A.H., P.J. Makovicky, and M.A. Norell. 2012. A review of dromaeosaurid systematics and paravian phylogeny. Bulletin of the American Museum of Natural History 371: 1–207.

Wang, L.L., et al. 2013. SIMS U-Pb zircon age of Jurassic sediments in Linglongta, Jianchang, western Liaoning: Constraint on the age of oldest feathered dinosaurs. Chinese Science Bulletin 58: 1346–1353. [in Chinese]

Wellnhofer, P. 1974. Das funfte Skelettexemplar von *Archaeopteryx*. Palaeontographica Abteilung A Palaeozoologie-Stratigraphie 147: 169–216.

Wellnhofer, P. 1988. Ein neues Exemplar von *Archaeopteryx*. Archaeopteryx 6: 1–30.

Wellnhofer, P. 1993. Das siebte Exemplar von *Archaeopteryx* aus den Solnhofener Schichten. Archaeopteryx 11: 1–48.

Wellnhofer, P. 2009. *Archaeopteryx:* the icon of evolution. Munich: Verlag F. Pfeil.

Witmer, L.M. 1997. The evolution of the antorbital cavity of archosaurs: a study in soft-tissue reconstruction in the fossil record with an analysis of the function of pneumaticity. Society of Vertebrate Paleontological Memoir 3: 1–73.

Xu, X. 2002. Deinonychosaurian fossils from the Jehol Group of western Liaoning and the coelurosaurian evolution. Ph.D. dissertation, Chinese Academy of Sciences, Beijing, China, 325 pp.

Xu, X., and M.A. Norell. 2004. A new troodontid dinosaur from China with avian-like sleeping posture. Nature 431: 838–841.

Xu, X., and F. Zhang. 2005. A new maniraptoran dinosaur from China with long feathers on the metatarsus. Naturwissenschaften 92 (4): 173–177.

Xu, X., X. Wang, and X. Wu. 1999. A dromaeosaurid dinosaur with a filamentous integument from the Jiufotang Formation of China. Nature 401: 262–266.

Xu, X., Z. Zhou, and X. Wang. 2000. The smallest known non-avian theropod dinosaur. Nature 408: 705–708.

Xu, X., M.A. Norell, X. Wang, P.J. Makovicky, and X. Wu. 2002. A basal troodontid from the Early Cretaceous of China. Nature 415: 780–784.

Xu, X., et al. 2003. Four-winged dinosaurs from China. Nature 421: 335–340.

Xu, X., et al. 2009. A new feathered maniraptoran dinosaur fossil that fills a morphological gap in avian origin. Chinese Science Bulletin 54: 430–435.

Xu, X., et al. 2010. A new dromaeosaurids (Dinosauria: Theropoda) from the Upper Cretaceous Wulansuhai Formation of Inner Mongolia, China. Zootaxa 2403: 1–9.

Xu, X., H. You, and F. Han. 2011. An *Archaeopteryx*-like theropod from China and the origin of Avialae. Nature 475: 465–470.

Xu, X., et al. 2012. The taxonomy of the troodontid IVPP V 10597 reconsidered. Vertebrata PalAsiatica 50 (2): 140–150.

Zanno, L.E., et al. 2011. A new troodontid theropod, *Talos sampsoni* gen. et sp. nov., from the Upper Cretaceous Western Interior Basin of North America. PLoS ONE 9 (6): e24487.

Zhang, F., Z. Zhou, X. Xu, and X. Wang. 2002. A juvenile coelurosaurian theropod from China indicates arboreal habits. Naturwissenschaften 89: 394–398.

Zhang, F., Z. Zhou, X. Xu, X. Wang, and C. Sullivan. 2008. A bizarre Jurassic maniraptoran from China with elongate ribbon-like feathers. Nature 455: 1105–1108.

Zhang, J., 2002. Discovery of the Daohugou biota (pre-Jehol biota) with a discussion of its geological age. Journal of Stratigraphy 26: 173–177.

Zheng, X., H. You, X. Xu, and Z. Dong. 2009. An Early Cretaceous heterodontosaurid dinosaur with filamentous integumentary structures. Nature 458: 333–336.

Zheng, X., et al. 2014. On the absence of sternal elements in *Anchiornis* (Paraves) and *Sapeornis* (Aves) and the complex early evolution of the avian sternum. Proceedings of the National Academy of Sciences 111 (38): 13900–13905.

Zhou, C. F., S. Wu., T. Martin, Z.X. Luo. 2013. A Jurassic mammaliaform and the earliest mammalian evolutionary adaptations. Nature 500: 163.

Zhou, Z., and F. Zhang. 2002. A long-tailed, seed-eating bird from the Early Cretaceous of China. Nature 418: 405–409.

Zhou, Z., and F. Zhang. 2003. Anatomy of the primitive bird *Sapeornis chaoyangensis* from the Early Cretaceous of Liaoning, China. Canadian Journal of Earth Sciences 40 (5): 731–747.

Zhou, Z., X. Wang. F. Zhang, and X. Xu. 2000. Important features of *Caudipteryx* – evidence from two nearly complete new specimens. Vertebrata Palasiatica 38 (4): 241–254.

APPENDIX 1

Abbreviation List

ar	articular
as	astragalus
atf	antorbital fenestra
ax	axis
bsr	basisphenoid recess
bt	basal tuber
btp	basipterygoid process
c	cervical vertebrae
ca	caudal vertebrae
dpc	deltopectoral crest
dr	dorsal rib
d.v.	dorsal vertebrae
fm	foramen magnum
fu	furcula
gtr	greater trochanter
hy	hyoid
lan	left angular
lc	left coracoid
ld	left dentary
lf	left femur
lfi	left fibula
lfr	left frontal
lep	left ectopterygoid
lh	left humerus
li	left ilium
lis	left ischium
lj	left jugal
llc	left lacrimal
l.m.	lepidosaur mandibles
lmx	left maxilla
ln	left nasal
lpa	left prearticular
lpm	left premaxilla
lpu	left pubis
lq	left quadrate
lra	left radius
lsa	left surangular
lsc	left scapular
lsp	left splenial
lti	left tibia
ltr	lessor trochanter
lu	left ulna
mc	metacarpal
mf	maxillary fenestra
m.o.	middle-ear opening
mt	metatarsal
ns	neural spine
oc	occipital condyle
op	olecranon process
p	parietal
pb	pubic boot
pl	palatine
po	postorbital
pmf	promaxillary fenestra
ptr	posterior trochanter
qj	quadratojugal
rad	radiale
ran	right angular
rc	right coracoid
rd	right dentary
rep	right ectopterygoid
rf	right femur
rfi	right fibula
rfr	right frontal
rh	right humerus
ri	right ilium
ris	right ischium
rj	right jugal
rlc	right lacrimal
rmx	right maxilla
rn	right nasal
rpm	right premaxilla
rpt	right pterygoid
rpu	right pubis
rq	right quadrate
rra	right radius
rsa	right surangular
rsc	right scapular
rti	right tibia
ru	right ulna
scr	subcondylar recess
sc.r.	sacral rib
sc.v.	sacral vertebrae
se	semilunate
so	supraoccipital
sq	squamosal
I-1	phalanx I-1

I-2	phalanx I-2
II-1	phalanx II-1
II-2	phalanx II-2
II-3	phalanx II-3
III-1	phalanx III-1
III-2	phalanx III-2
III-3	phalanx III-3
III-4	phalanx III-4
IV-1	phalanx IV-1
IV-2	phalanx IV-2
IV-3	phalanx IV-3
IV-4	phalanx IV-4
IV-5	phalanx IV-5
X	cranial nerve opening X
XI	cranial nerve opening XI
XII	cranial nerve opening XII

Scientific Publications of the American Museum of Natural History

American Museum Novitates
Bulletin of the American Museum of Natural History
Anthropological Papers of the American Museum of Natural History

Publications Committee
Robert S. Voss, Chair

Board of Editors
Jin Meng, Paleontology
Lorenzo Prendini, Invertebrate Zoology
Robert S. Voss, Vertebrate Zoology
Peter M. Whiteley, Anthropology

Managing Editor
Mary Knight

Submission procedures can be found at http://research.amnh.org/scipubs

All issues of *Novitates* and *Bulletin* are available on the web (http://digitallibrary.amnh.org/dspace). Order printed copies on the web from:
http://shop.amnh.org/a701/shop-by-category/books/scientific-publications.html

or via standard mail from:

American Museum of Natural History—Scientific Publications
Central Park West at 79th Street
New York, NY 10024

♾ This paper meets the requirements of ANSI/NISO Z39.48-1992 (permanence of paper).

On the cover: BMNHC PH804, referred specimen of *Anchiornis huxleyi,* collected by the Beijing Museum of Natural History.